


Osteoclast-expanded supercharged NK cells perform superior antitumour effector functions

Meng-Wei Ko,¹ Ao Mei,^{2,3} Emanuela Senjor,^{1,4,5} Milica Perišić Nanut,⁴ Lucy Wanrong Gao,⁶ Paul Wong,¹ Po-Chun Chen,¹ Whitaker Cohn,⁶ Julian P Whitelegge,⁶ Janko Kos,^{4,5} Kawaljit Kaur ,¹ Subramaniam Malarkannan,^{2,3} Anahid Jewett^{1,7}

To cite: Ko M-W, Mei A, Senjor E, *et al.* Osteoclast-expanded supercharged NK cells perform superior antitumour effector functions. *BMJ Oncology* 2025;**4**:e000676. doi:10.1136/bmjonc-2024-000676

► Additional supplemental material is published online only. To view, please visit the journal online (<https://doi.org/10.1136/bmjonc-2024-000676>).

M-WK and AM contributed equally.

Received 29 January 2025
Accepted 28 April 2025



► <https://doi.org/10.1136/bmjonc-2025-000857>



© Author(s) (or their employer(s)) 2025. Re-use permitted under CC BY-NC. No commercial re-use. See rights and permissions. Published by BMJ Group.

For numbered affiliations see end of article.

Correspondence to
Dr Anahid Jewett;
ajewett@mednet.ucla.edu and
Dr Subramaniam Malarkannan;
smalarka@mcw.edu

ABSTRACT

Objective Natural killer (NK) cells are the largest innate lymphocyte subset with potent antitumour and antiviral functions. However, clinical utilisation of human NK cells is hampered due to a lack of reliable methods to augment their antitumour potential. We demonstrated technology in which human NK cells were cocultured with osteoclasts in the presence of probiotic bacteria. This approach significantly augmented the antitumour cytotoxicity and polyfunctionality of human NK cells, resulting in the generation of supercharged NK (sNK) cells.

Methods and analysis We explored the proteomic, transcriptomic and functional characterisation of sNK cells using cell imaging, flow cytometric analysis, 51-chromium release cytotoxicity assay, ELISA, ELISPOT, IsoPLEXIS single-cell secretome analysis, proteomic analysis, RNA analysis, western blot and enzyme kinetics.

Results We found that sNK cells were less susceptible to split antigen and tumour-induced exhaustion. Proteomic analyses revealed that sNK cells significantly increased their cell motility and proliferation. Single-cell transcriptomes uncovered sNK cells undertaking a unique differentiation trajectory and turning on STAT1, JUN, BHLHE40, ELF1, MAX and MYC regulons essential for augmenting antitumour effector functions and proliferation, respectively. Both proteomic and single-cell transcriptomes revealed that an increase in Cathepsin C helped to augment the quantity and function of Granzyme B.

Conclusions These results support that this unique method produces potent NK cells for clinical utilisation and delineate the molecular mechanisms associated with this process.

INTRODUCTION

Natural killer (NK) cells are the major effector cells in the innate immune system. NK cells mediate cytotoxicity and regulate innate and adaptive immune functions by releasing proinflammatory and anti-inflammatory cytokines and chemokines.¹ NK cells mediate direct cell lysis in response to the sum of activating and inhibitory signals received on cell-cell interaction via immune synapses.² The loss of the self-identification

WHAT IS ALREADY KNOWN ON THIS TOPIC

⇒ Due to their immunosurveillance capability and ability to target the most aggressive stem-like tumours, which give rise to metastatic tumours, Natural killer (NK) cells have great potential to be clinically used. However, the major limitations in using NK cells in clinical trials include a lack of approaches to augment their expansion and anti-tumour effector functions and sustain their longevity and persistence in vivo.

WHAT THIS STUDY ADDS

⇒ Thus, to overcome these limitations, we previously established a method to significantly increase the antitumour functions of human NK cells, which we named 'supercharged' NK (sNK) cells. The current study uses proteomic, transcriptomic and functional analyses to define the molecular mechanisms by which sNK cells function. We found that the sNK cells have upregulated the protein levels of activating/costimulatory receptors, decreased the expression of integrins required for tissue localisation, upregulated genes necessary for active proliferation, upregulated their capabilities to be polyfunctional and were not subjected to split antigen or exhaustion. We identify AP1 regulons-based transcriptional networks from single-cell transcriptomes responsible for the enhanced effector functions in sNK cells. We also define a post-translational mechanism that increases the activity of Granzyme B by interactions between Cathepsin C and Cystatin F.

HOW THIS STUDY MIGHT AFFECT RESEARCH, PRACTICE OR POLICY

⇒ sNK cells will be highly effective for use in clinical trials of liquid and solid tumours.

molecule (MHC class I), which binds to the inhibitory receptors on NK cells, triggers the NK cell-mediated cytotoxic function and ultimately releases cytotoxic granules containing perforin and granzyme B. This results in the induction of cell death and lysis of the target cells.³

Importantly, NK cells shape the tumour microenvironment and halt the tumour progression.⁴ They eliminate cancer stem cells (CSCs) through direct lysis and differentiate malignant cells through cytokine secretion, leading to the curtailment of tumours.⁵ NK cells produce cytokines, such as IFN- γ and IFN- α ; these cytokines play a crucial role in differentiating stem-like target cells.⁶ Our laboratory has previously identified various surface markers to determine the differentiation status of tumour cells, including CD44, CD54, B7H1 (PD-L1) and MHC class I.⁷ Moreover, NK-differentiated CSCs are more sensitive to chemotherapeutic and radiotherapeutic drugs.⁸ However, the functions of NK cells are ineffective in cancer patients and during preneoplastic and neoplastic stages in mice.^{4,9} In these circumstances, NK cells have less cytotoxicity and do not secrete sufficient quantities of cytokines. These NK cell dysfunctions are associated with increased cancer risk, higher chances of metastasis and poor prognosis for cancer patients. Due to the dysregulated functions, an immunotherapy engineered to improve NK cell antitumour functions in cancer patients is urgently needed.

Cancer immunotherapy clinical trials have shown efficacy in several types of cancer, including lymphoid tumours, breast cancer and colorectal cancer.^{10–14} NK cell-based immunotherapy clinical trials have demonstrated therapeutic benefits against several cancers,¹⁵ including multiple myeloma,¹⁶ hepatocellular carcinoma,¹⁷ AML,¹⁸ digestive cancer¹⁹ and osteosarcoma.²⁰ However, getting functionally competent NK cells, scalability, persistence and withstanding the suppressive nature of the tumour microenvironment are all factors that influence the success of the clinical trials and are lacking in many NK cell therapeutics.

To overcome the negative factors that influence the success of NK cell immunotherapy, we have previously established a novel strategy to expand NK cells with potent abilities, deeming them ‘supercharged’ NK (sNK) cells.^{7,21} In this expansion process, primary NK cells are purified from the peripheral blood and treated with IL-2 and anti-CD16 monoclonal antibodies (mAbs) overnight before coculture with the feeder cells, osteoclasts (OCs) and sonicated probiotic bacterial preparation called sAJ2.⁷ After receiving the signals from cell–cell interaction, surface receptor crosslinking, and cytokine stimulation, NK cells exhibit a high proliferation rate, increased cytotoxicity and augmented cytokine secretion. Furthermore, these cells demonstrated great therapeutic potential in cancer immunotherapy with exceptional ability to limit tumour growth and improve the immune system and efficacy of immunotherapy in the oral and pancreatic tumour-bearing humanised bone marrow/liver/thymus (BLT) (hu-BLT) mice model.⁷

The current study defines how sNK cells mediate their effector functions using single-cell transcriptome, proteome and functional experiments evaluating their cytotoxicity and cytokine secretion. Using proteomic data, we found sNK cells significantly reduced ITGAL (LFA1),

ICAM2, ITGB1 (CD29), ITGB3 (GPIIIa) and several intracellular signalling proteins (RAP1B, RAPIGAP2, FERMT3) that are located downstream of these integrins compared with cultured primary NK (pNK) cells. This finding suggests that sNK cells are migratory and less tissue-resident. In contrast, sNK cells significantly upregulated activating or co-receptors, including CD2, CD44, CD48, CD53, CD59 and CD63, indicating an ‘altered balance’ that leads to high motility and antitumour cytotoxic functions.²² Both proteomic and single-cell transcriptomic data suggested that sNK cells are highly proliferative with augmented protein translation. Single-cell RNA sequencing revealed that sNK cells exhibit a distinct transcriptome, developmental progression and gene regulatory network (GRN) compared with cultured pNK or freshly isolated peripheral blood NK cells. sNK cells were polyfunctional, produced significant quantities of inflammatory cytokines and mediated strong anti-tumour responses without being subjected to split anergy.²³

Mechanistically, post-translational regulation of cleaving pro-Granzyme B to functional Granzyme B by Cathepsin C forms the basis for the increased cytotoxic potential of sNK cells. Cathepsin C converts pro-Granzyme B to active Granzyme B, whereas Cathepsin L activates perforin. The activity of cathepsins is negatively regulated by cystatins, among which Cystatin F is particularly important in immune cells, as it inhibits the activity of both Cathepsin C and L. We found increased expression of inactive dimeric Cystatin F with higher molecular weight and altered glycosylation profile in sNK cells compared with pNK cells, which may have an impact on the sNK cell cytotoxicity via the regulation of the activity of Cathepsin C.^{24–27} In addition, an augmented expression and function of STAT1 and STAT4 formed the basis for increased sNK cell proliferation and their ability to produce significantly higher amounts of proinflammatory cytokines. We further demonstrate that sNK cells maintained their potent effector function after encountering tumour cells, providing a promising therapeutic benefit in vivo and an option for cancer immunotherapy. Collectively, our results provide a novel approach to enhancing and sustaining antitumour effector functions of human NK cells using OCs cultured with a combination of probiotic bacteria.

RESULTS

OC-induced sNK cells are phenotypically distinct from IL-2-only cultured pNK cells

The sNK cells were generated using the previously established protocol as described in the Materials and Methods section.^{5,7,21,28} Briefly, freshly isolated NK cells were treated with recombinant human IL-2 and anti-CD16 mAbs. After 18 hours, IL-2 and anti-CD16 mAbs-activated NK cells were cocultured with OCs and sonicated probiotic AJ2 bacteria (sAJ2) for 21 days and used. sNK cells were larger and polymorphic than only IL-2-cultured primary NK (pNK)

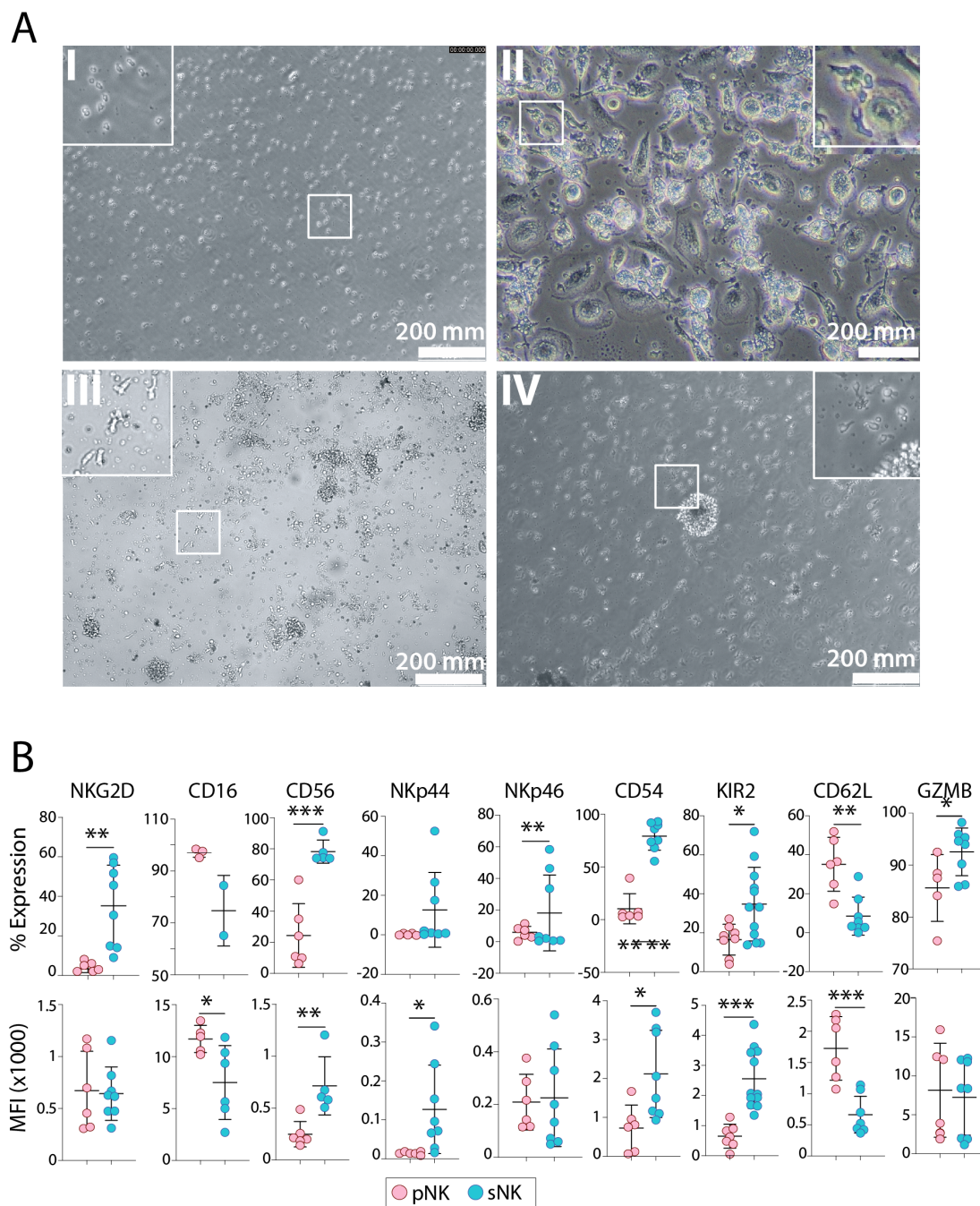


Figure 1 The use of osteoclasts and probiotic bacteria to generate highly active supercharged natural killer (sNK) cells. (A) Changes in the morphological features of NK cells during the expansion of sNK cells using osteoclasts and probiotic bacteria. Primary NK (pNK) cells were freshly isolated from PBMCs. Multinucleated osteoclasts (OCs) were differentiated from peripheral blood-derived monocytes for 21 days with M-CSF and RANK-L. (I) pNK cells on Day 1. (II) IL-2 and anti-CD16 mAb-treated pNK cells are attached to the osteoclasts after overnight coculture with OCs. (III) After 5 days of coculture, OCs were not present in the culture, and NK cells became larger, elongated, irregularly shaped and started to form clusters. (IV) At the prime expansion period (day 7 and after) for sNK cells proliferate in both floating and attaching clumps in the cell culture. (B) Phenotypic analyses of pNK and sNK cells were performed after 7 days of treatment with IL-2 (1000 U/mL) using flow cytometry analysis. Per cent expression and mean fluorescence intensity of NKG2D, KIR2, Nkp44, Nkp46, CD54, CD62L, CD16, CD56 and GZMB are shown. For gating strategies, please see online supplemental figure S1. M-CSF, macrophage colony-stimulating factor. * (p-value < 0.01-0.05), ** (p-value < 0.01-0.001), *** (p-value < 0.001-0.0001), **** (p-value < 0.00001)

cells. Even though the irregular elongated cells can occasionally be spotted in pNK cells, they are usually uniformly round in shape (figure 1A, panel I). At the start of the culture, sNK cells attached to the feeder cells, the mature

OCs, layering at the bottom of the cell culture plate, and started to form clusters (figure 1A, panel II). OCs are no longer present between 5 and 7 days of the culture. sNK cells became elongated and polymorphic with more

granules, notably larger than pNK cells (figure 1A, panel III). From day 7 to day 21, sNK cells expand in clusters, attaching to the plate or floating in the culture medium (figure 1A, panel IV).

To further define the phenotypical differences between sNK and pNK cells, we measured several cell surface markers using flow cytometry (figure 1B). Either per cent positive population or mean fluorescence intensity (MFI) showed that both activating and inhibitory receptors, including NKG2D, NKP44, NKP46, CD54 and KIR2, were found to be higher in sNK than pNK cells; while L-selectin (CD62L) was lower in sNK cells. It is worth noting that when the human NK cell stage-identifying receptors, CD56 and CD16, were measured, CD56 was expressed higher in sNK cells while CD16 expression was decreased, which could be potentially caused by the anti-CD16 mAbs treatment. Furthermore, intracellular staining of Granzyme B, which is one of the important molecules of NK cells in granule-mediated cytotoxicity, is more prominent in sNK cells (figure 1B). The gating strategy of the data shown in figure 1B is shown in online supplemental figure S1. We conclude that the OCs-induced sNK cells are morphologically and phenotypically different from pNK cells, with more cytolytic molecules produced.

sNK cells exhibit increased protein translation, cell proliferation and decreased cell motility

Next, we sought to determine the proteomic differences between pNK and sNK cells. Towards this, we investigated qualitative and quantitative differences in their protein expressions using bulk proteomic mass spectrometry analysis. The fold changes in protein abundance of sNK over pNK were calculated across donors or within the same donors (figure 2A,B). Between different donors, we found that 90 proteins were more abundant in sNK cells, while 21 proteins were less abundant (figure 2A). When compared within the same donors, we observed increases in the abundance of 271 proteins and decreases in 172 proteins in sNK cells (figure 2B). Among these, we found three major biological processes. First, proteins associated with actin cytoskeleton organisation were significantly downregulated in sNK cells (figure 1A). Particularly, several integrins, including ITGA2B, ITGA6, ITGB3 and ICAM2 were reduced in sNK cells compared with pNK cells (figure 2C). Apart from these, the quantities of signalling proteins downstream of integrins that are involved in 'inside-out' signalling (RAP1GAP2, RAP1B and FERMT3), were also reduced in sNK cells. The reductions in the protein quantity of ITGA6 and ITGB3 strongly imply that sNK cells actively reduced their interactions with the extracellular matrix and are highly motile, which could be correlated with the morphological alterations of sNK cells. Reductions in ITGA2B, ICAM2 and 'inside-out' signalling molecules imply functional changes in sNK cells.

Second, sNK cells significantly upregulated SLAM family members CD2 and CD48, while the third member CD84 was downregulated. These cell surface receptors

primarily serve as activating or costimulatory receptors. We found tetraspanin family members CD53 and CD63 (granulophysin) were upregulated, while the third member, CD9, was unaltered (figure 2D). Homotypic interaction of CD53 between NK cells is known to augment their proliferation significantly.²⁹ CD44, a receptor that binds to multiple soluble or matrix-located ligands and promotes cell proliferation, was also increased in sNK compared with the pNK cells. CD59, a GPI-anchored glycoprotein, also increased in sNK cells, is a coreceptor for NKP46 (NCR1) and NKP30 (NCR3) that augments NK cell-mediated cytotoxicity.³⁰ These results imply that protein expression of several activating receptors was significantly increased in sNK cells, potentially facilitating their augmented antitumour cytotoxicity.

The last set of proteins that were upregulated in sNK cells relates to cell proliferation. Consistent with the previous report data of fast-expanding sNK characteristics,⁷ sNK cells expressed higher levels of cell proliferation marker MKI67 than pNK (online supplemental figure S2A–C). Moreover, in proteomic analysis, sNK showed more abundant cell proliferation proteins, for example, minichromosome maintenance proteins (MCMs) and KI67 (online supplemental figure S2D). To gain further insights into the proliferative capacity of sNK cells, we conducted a cell-cycle score analysis on the single-cell RNA sequencing data. This revealed that a considerably higher proportion of sNK cells were in the G2M phase, indicating an enhanced proliferation programme in these cells compared with pNK cells (online supplemental figure S2E). Moreover, we observed higher expression of cell cycle-associated genes, including MKI67, E2Fs and MCMs, in sNK cells (online supplemental figure S2F). Notably, this active proliferative state was still regulated by the upregulation of TP53 and its associated components, which are essential for maintaining genomic integrity (online supplemental figure S2G). Consistent with these findings, protein-level analyses revealed that the proliferation marker MKI67 and MCMs, essential for DNA replication, are significantly upregulated in sNK cells compared with pNK cells (online supplemental figure S2F–H). Our results suggest that sNK cells exhibit a more proliferative state than pNK cells, which may contribute to their enhanced antitumour activity. These data verified our previous finding and confirmed that sNK cells are more proliferative than pNK in surface protein, total protein and RNA expression levels. In summary, sNK cells have a distinct proteomic profile compared with pNK cells, with translational upregulation of molecules for proliferation and effector function activities.

By applying protein set enrichment assay (PSEA), we found multiple pathways related to ribonucleoprotein formation, mRNA processing and translation, and cell proliferation, implying sNK cells are in a more functionally active state (figure 2E). The reduction in integrin proteins was also reflected in the PSEA plot as both actin cytoskeleton organisation and cell motility were significantly less in sNK cells (figure 2E). Besides actin

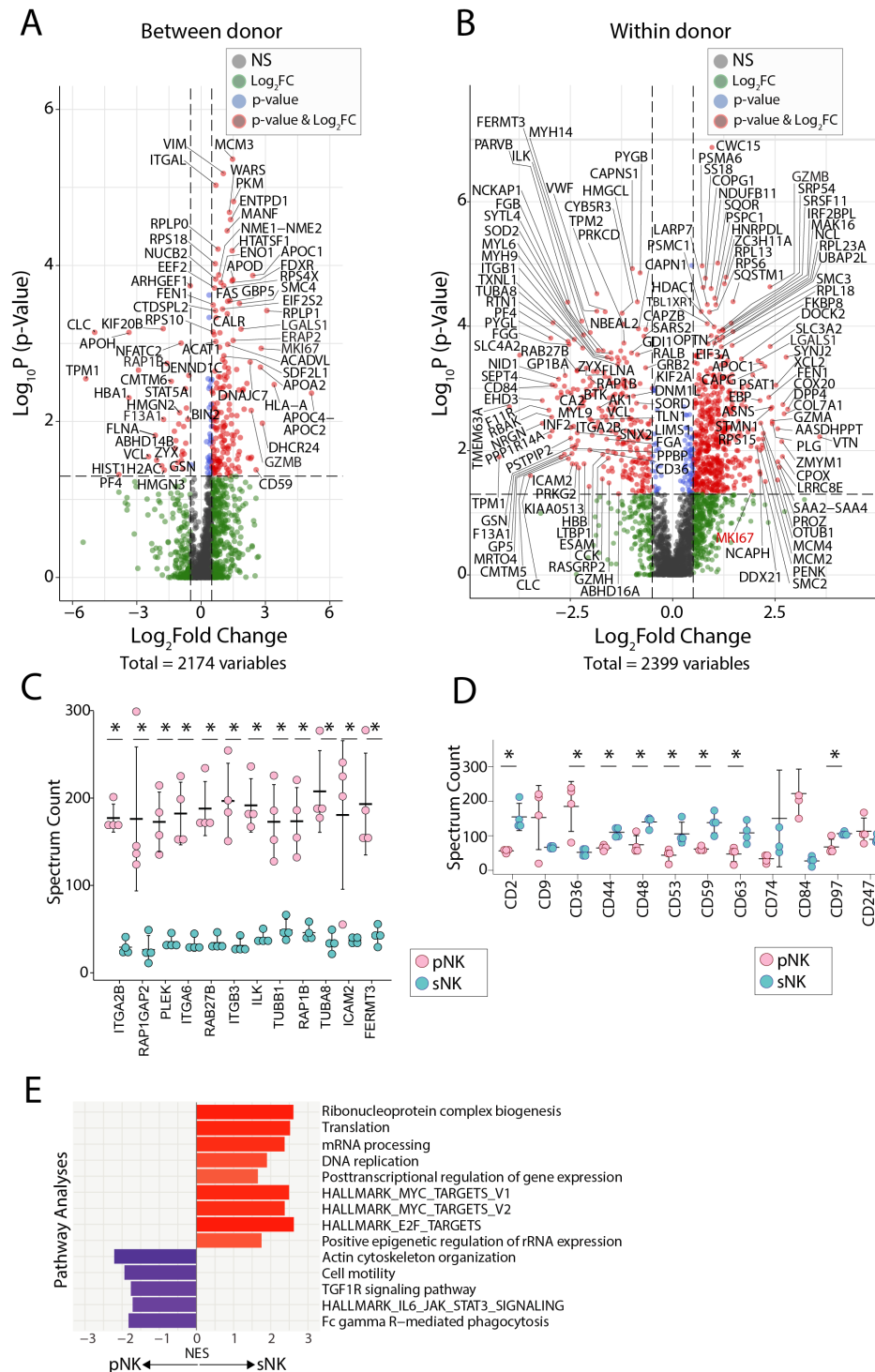


Figure 2 Supercharged natural killer (sNK) cells exhibit increased protein translation, cell proliferation and decreased cell motility. Mass spectrometric analyses were performed to identify the proteomic differences. Primary NK (pNK) or sNK cells (2×10^6 each) were used for proteomic analysis. Red dots show the fold change of protein abundance of sNK cells/IL-2 treated pNK cells is greater than 0.5 and with statistical significance ($n=90$ (A), 271 (B), $p<0.05$) and blue dots indicate the fold change of protein abundance is of sNK cells/pNK cells less than 0.5 ($n=21$ (A), 172 (B), $p<0.05$) with statistical significance ($p<0.05$). The comparison of primary and sNK cells obtained from different donors is shown in (A), and from the same donors is shown in (B). Proteins with abundance alterations between primary and sNK cells within the same donors were selected and categorised according to their biological function. Paired t-test were performed to determine the statistical differences ($n=4$, $*p<0.05$), (C,D). PSEA analyses revealed altered functional pathways between pNK and sNK cells. Quantitative differences is shown in integrins and their downstream signalling molecules between pNK and sNK cells. PSEA, protein set enrichment assay (E).

cytoskeleton organisation and cell motility pathways, TGF1R and IL-6 signalling pathways, which have been shown to hinder the effector function of NK cells, are downregulated in sNK cells (figure 2E).

Single-cell RNA sequencing reveals sNK cell heterogeneity and its distinct transcriptional landscape

Besides the proteomic analysis, we also used 10X single-cell RNA sequencing technology to evaluate transcriptomic differences at the single-cell level in these NK cells. Specifically, we aimed to understand the underlying mechanism of the functional differences between sNK cells and IL-2-treated pNK cells. To facilitate the analysis and the categorisation of NK cell subsets, we included untreated NK cells derived from donor PBMC (HC-NK) in our study.³¹ After filtering, 11 824 cells (2,944 sNK cells and 8880 pNK cells) were analysed. We identified four transcriptionally distinct NK cell clusters among HC-NK (untreated pNK), pNK (IL-2 treated pNK) and sNK cells (figure 3A,B). Clusters #1, #2, #3 and #4 were present in untreated and IL-2-treated pNK cells. In contrast, sNK cells only showed clusters #1, #2 and #3 (figure 3C). According to the top genes expressed across each cluster (figure 3D), cluster #1 resembles the previously described CD56^{Bright} NK cells with the highest expression of *SELL*, *LTB* and *GZMK*.^{31 32} Cluster #2 follows a subset of transitional NK cells between CD56^{Bright} and CD56^{Dim} NK cells, upregulating genes necessary for NK cell maturation, such as *IER3* and *JUNB*.³¹ Chemokines (*CCL3*, *CCL4*, *CCL5*) and cytolytic molecule (*GZMA*, *GZMB*, *PRF1*) genes are significantly higher in cluster #3, indicating their identity as cytotoxic CD56^{Dim} NK cells. Cluster #4 expressed more genes associated with an inactive state of NK cells, which could be identified as terminal NK cells. When compared with untreated and IL-2-cultured pNK cells, sNK cells had higher *CCL3*, *JUN*, *ID2*, *IFNG*, *NCAM1* and *GNLY* expression, with lower expression of *KLRF1*, *KLRC1*, *KLRD1* and *GZMH* (figure 3E,F). To further identify the uniqueness of sNK cells, we analysed additional transcripts. We found *IL2RB* (CD122), *NKG7*, *FCGR3A* and *CD7* were significantly lower in sNK compared with untreated or IL-2-treated pNK cells (figure 3E,F). We used the Gene Set Enrichment Analyses (GSEA) to investigate potential cellular signalling pathways (figure 3G). Gene sets representing cell proliferation were upregulated in sNK cells (Positive regulation of cell cycle, negative regulation of apoptotic signalling pathway, Hallmark gene set of E2F targets, and Hallmark gene set of MYC targets V1/V2). In addition, multiple gene sets representing cellular activation were also upregulated in sNK cells (figure 3G). Moreover, numerous pathways representing activation (ERK1/2 cascade, Positive regulation of MAPK cascade, JNK cascade, MTORC1, Glycolysis and NF-κB signalling pathway) were found in sNK cells using multiple GSEA database (online supplemental figure S3A–C). Our findings suggest that sNK cells are transcriptionally distinct from untreated or IL-2-treated pNK cells.

sNK cells follow a distinct developmental trajectory

To determine the mechanism involved in the unique development or differentiation of sNK cells, we employed Monocle2-based pseudotime trajectory analysis (figure 4A). Computational ordering of cells in an unsupervised manner using maximal transcriptional similarity between successive pairs of cells allowed us to define the transcriptomic continuity of NK cells. We compared the trajectories of pNK (IL-2-treated pNK) and sNK to freshly derived human HC NK (untreated pNK) cells (figure 4B). Pseudotime ordering formed a gradual progression of differentiating NK cells from the point of origin. Based on their transcriptomic continuity, the four clusters were located in distinct places (figure 4A). NK cells in cluster #1 formed the origin in all three samples. This is consistent with its transcriptomic profiles, expressing immature CD56^{Bright} NK cell markers, including *SELL*, *LTB* and *GZMK*. Continuous expression resolution of DEGs at BP1 by temporal topologies of NK cells using the BEAM (branched expression analysis modelling) approach in Monocle2 allowed us to determine whether a gene is associated with this BP1 bifurcation node (figure 4C). Cluster #1 progressed to a branch point (BP1), which split the progression into two distinct cell fate decisions (C_F1 and C_F2) (figure 4B). Cluster #2 is present in all three samples, forming a bridge to cluster #3 and #4, which constituted the terminal differentiation of NK cells in both untreated pNK and sNK cells but not in IL-treated pNK cells. Cluster #4 is present only in HC and pNK cells but not in sNK. Among pNK cells, clusters #2, #3 and #4 were dispersed throughout the developmental axis, indicating that culturing NK cells with IL-2 results in a more mixed transcriptomic profile and it does not support an orderly transition of NK cells (figure 4B, middle panel). In contrast, clusters #3 and #4 in fresh untreated pNK cells exhibited transcriptomically mature phenotype (figure 4B, left panel). Importantly, the cell fates of sNK and untreated pNK were opposite, resulting in them at C_F1 and C_F2, respectively (figure 4B, left and right panels).

Given that clusters #2, #3 and #4 in pNK cells were not transcriptomically distinct, we chose untreated pNK cells to compare with sNK cells for further cell fate decision analyses. First, we analysed the gene expressions at the BP1 (figure 4C). Cells at BP1 move towards either C_F1 or C_F2. Gene expression profile at BP1 provides a snapshot of the maturity of cells. We found *XCL1*, *CXCR4*, *CXCR5*, *GZMK* and *LTB* transcripts in NK cells at BP1, which define these cells as CD56^{Bright}, consistent with the notion that the pseudotime trajectory starts with immature NK cells. Next, we analysed the gene expression in cells moving towards C_F1 in HC-NK cells. At the start of the BP1, these cells started expressing *GZMA*, *CTSC*, *CCL4*, *XCL2*, *GZMH*, *PRF1*, *GZMB* and *CST7* (figure 4C). However, their expressions were undetectable, indicating that the cells at the end of the trajectory became non-cytotoxic. In contrast, at the end of the trajectory, sNK cells expressed high transcripts encoding *CCL5*, *CCL4*,

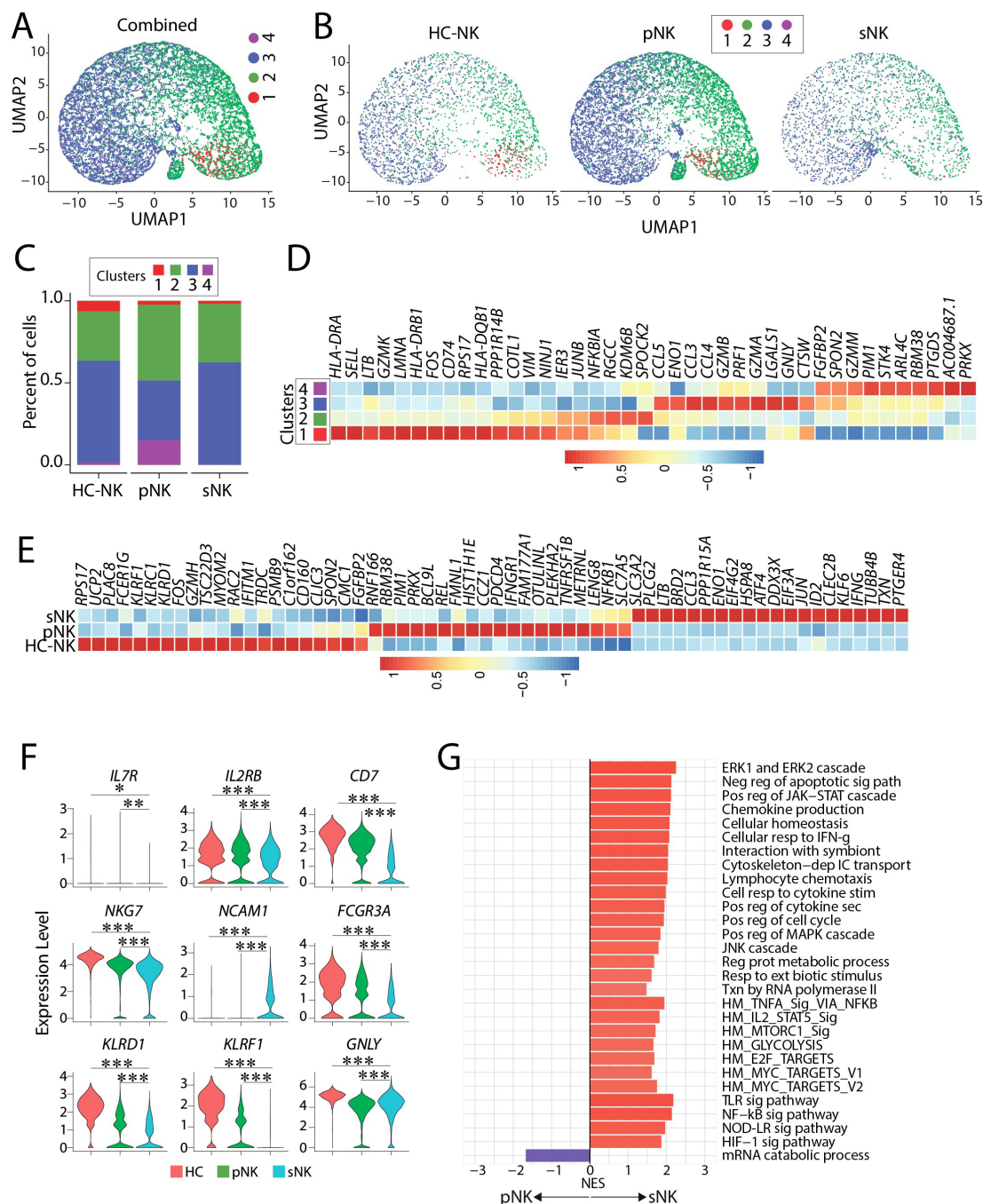


Figure 3 Single-cell RNA (scRNA) sequencing identifies a unique transcriptome in supercharged natural killer (sNK) cells. (A) Identification of transcriptomically distinct cell clusters as depicted by UMAP of combined Healthy control-NK ved (HC-NK (untreated primary NK (pNK)), pNK (IL-2 treated pNK) and sNK cells. (B) Individual UMAPs of HC-NK (untreated pNK), pNK (IL-2 treated pNK) and sNK cells. (C) The percentages of individual clusters in HC-NK (untreated pNK), pNK (IL-2 treated pNK) and sNK cells. (D) Top cluster-defining genes indicate the uniqueness of each cluster. (E) Gene signatures of HC-NK (untreated pNK), pNK (IL-2 treated pNK) and sNK cells. (F) Violin plots of genes representing the developmental and functional status of NK cells among HC-NK (untreated pNK), pNK (IL-2 treated pNK) and sNK cells. (G) Major signalling pathways based on gene set enrichment analyses are distinctly operating in sNK cells compared pNK (IL-2 treated pNK) cells. UMAP, Uniform Manifold Approximation and Projection. *(p-value < 0.01-0.05), ***(p-value < 0.001)

IFNG, *CCL3*, *TNF* and *CSF1* (figure 4C). sNK cells also expressed only moderate *GZMA*, *GNLY*, *PRF1* and *GZMB* transcript levels. To further validate our scRNA-seq data, we performed bulk RNA sequencing of total IL-2-treated pNK or sNK cells. We found higher *IFNG* and *TNF*

(figure 4D). However, we did not observe dramatic differences in the transcript levels of *GZMB* and *PRF1*.

Next, we defined the regulons to identify the GRNs involved with sNK cells. We employed a single-cell regulatory network inference and clustering (SCENIC) analysis

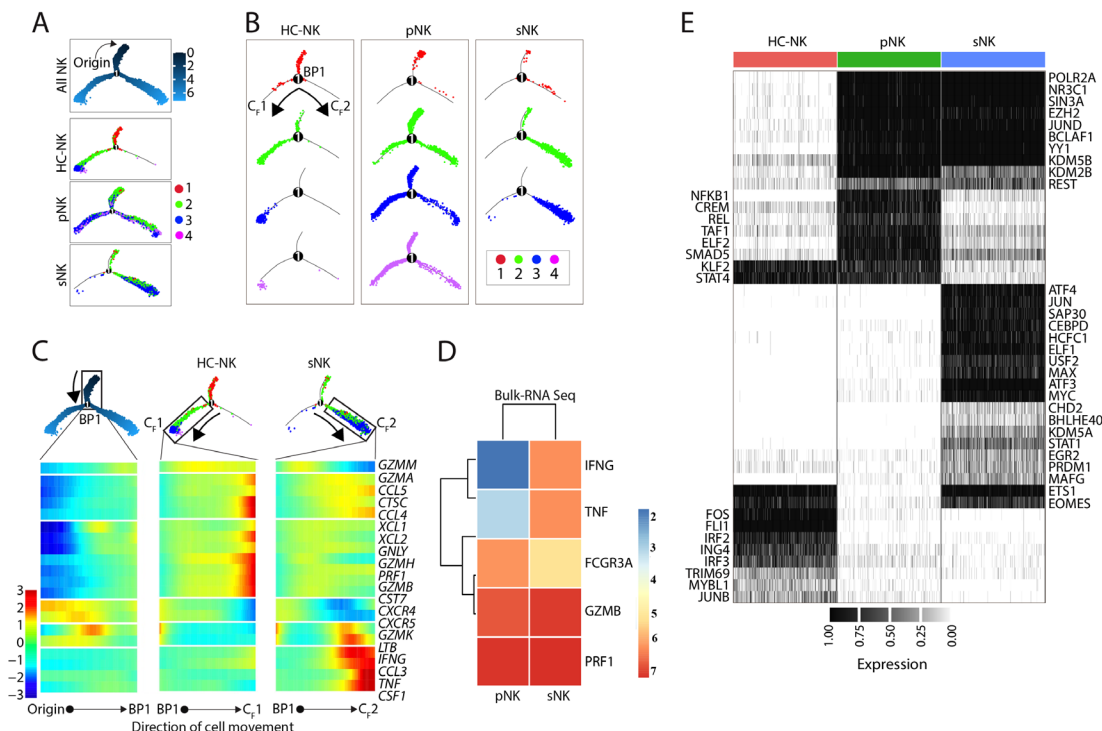


Figure 4 Supercharged natural killer (sNK) cells follow a distinct developmental trajectory. (A) Monocle2-based cell trajectory analyses of combined Healthy control NK (HC-NK) (untreated primary NK (pNK)), pNK (IL-2 treated pNK) and sNK cells (Top). The start of the trajectory 'origin' is indicated. Locations of individual clusters in the trajectory (bottom) are shown for HC-NK (untreated pNK), pNK (IL-2 treated pNK) and sNK cells. The colour bar indicates the pseudotime progression. (B) Trajectory analyses of individual NK clusters. Branch point-1 (BP1) and the endpoint cell fates, C_F1 and C_F2, are marked. (C) The heatmap of gene expression for each cell across pseudotime representing BP1 for all NK cells, C_F1 for HC-NK (untreated pNK), pNK (IL-2 treated pNK) and C_F2 for sNK cells. The x-axis of the heatmaps represents the pseudotime trajectory ordering of individual cells. Z-scale with colour intensity represents the levels of transcripts in each cell. A centre box in the middle of the left panel represents the cells at BP1. The direction of cell predicted cell movement is marked as BP1 to C_F1 (middle panel), and BP1 to C_F2 (right panel). (D) Relative transcript levels of indicated genes from bulk-RNA sequencing. (E) The regulon activity present in HC-NK (untreated pNK), pNK (IL-2 treated pNK) and sNK cells. Each column represents a single cell. The regulon names and the number of target genes for each regulon are shown. Grey and black Z-scale indicate the level of regulon activity in individual cells.

for this. Each transcription factor regulates multiple target genes grouped into units referred to as regulons. We identified target genes regulated by a transcription factor identified from motif enrichment analyses using the GRNboost2 fast GRN algorithm.³³ Regulon activity was calculated for HC-NK, pNK, and sNK cells.³⁴ The ranked distribution of AUCell scores across individual cells from a binary output determined the threshold for active and inactive regulons. This analysis identified 45 co-regulated regulons (figure 4E and online supplemental figure S4). As expected, untreated pNK and sNK cells possessed minimal shared regulons (ETS1 and EOMES). However, the IL-2-treated pNK and the sNK cells shared a considerable number of regulons (POLR2A, NR3C1, SIN3A, EZH2, JUND, BCLAF1, YY1, KDM5B, KDM2B and REST). 17 regulons were uniquely operating in sNK cells, and among these, ATF4, JUN, ATF3 and MAFG transcription factors belong to the Activation protein-1 (AP1) family.³⁵ ELFI, MAX and MYC regulons represent the GRNs governing heightened cell proliferation of sNK cells. MAX and BHLHE40 transcription factors belong to basic helix-loop-helix transcription factors (bHLH), and

their downstream target genes primarily regulate lymphocyte effector functions in sNK cells. STAT1, a downstream target of IFN- γ , potentially represents an autocrine activation of sNK cells, a mechanism upregulating cathepsins.³⁶ Increased activities of ATF3, ATF4 and PRDM1 regulons imply increased regulatory transcriptional networks that operate on inflammatory cytokine production. These results strongly suggest that the sNK cells possess a distinct developmental trajectory governed by unique sets of gene expressions regulated by a discrete set of regulons.

sNK cells are cytotoxic, produce high IFN- γ and are not constrained by split anergy

The conventional cytotoxic NK cells (CD16⁺CD56^{dim}) lyse less differentiated cancer cells by recognising the lack of the MHC I molecule.^{37 38} However, split anergy-stage NK cells (CD16⁺CD56^{Bright}) secrete cytokines (mainly IFN- γ and TNF- α) to differentiate CSCs.²³ IL-2 and anti-CD16 antibody treatment induce the split anergy stage, transitioning NK cells from cytotoxic to potent cytokine-secreting.^{1 23} Therefore, we first compared the cytotoxic potentials of IL-2-treated pNK and sNK cells. We found

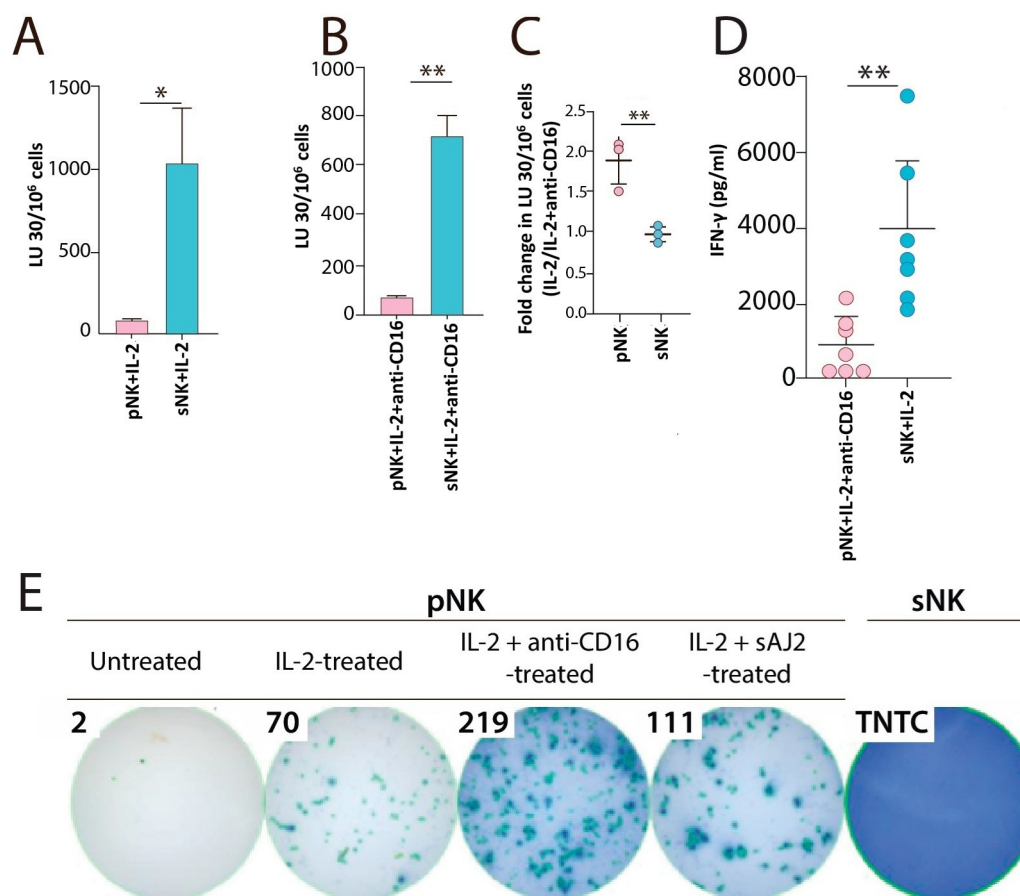


Figure 5 Supercharged natural killer (sNK) cells are cytotoxic, produce high IFN- γ and are not constrained by split anergy. Primary NK (pNK) cells were freshly purified from peripheral blood-derived mononuclear cells (PBMCs). pNK and sNK cells were treated with IL-2 for 18–24 hours before the supernatant was collected. 51 chromium release assay was performed to determine the cytotoxicity of NK cells against OSCSCs, and lytic unit 30 (LU30/10⁶ cells) was calculated accordingly. (A) IL-2-activated pNK and IL-2 treated sNK, (B) IL-2+ anti-CD16 mAbs activated pNK and IL-2+anti-CD16 mAbs activated sNK (n=3). (C) Fold decrease in cytotoxicity (IL-2+anti-CD16 mAbs/IL-2) was calculated using the lytic unit 30 (D). ELISA was used to assess the levels of IFN- γ released in the culture supernatant IL-2 and anti-CD16 mAbs activated pNK and IL-2 activated sNK (n=7). (E) Elispot was performed to determine the relative number of cells secreting IFN- γ , shown as spot counts. TNTC, too numerous to count. * (p-value < 0.01–0.05), ** (p-value < 0.01–0.001), *** (p-value < 0.001)

IL-2-treated sNK cells have profound cytotoxicity against poorly differentiated cancer cells, such as oral squamous CSCs (OSCSCs), compared with IL-2-activated pNK cells (figure 5A). Next, we sought to investigate if these sNK cells can also be induced into the split anergy stage through treating both pNK and sNK cells with IL-2 and anti-CD16 mAbs. After the split anergy induction treatment (IL-2 and anti-CD16 antibody), sNK cells still displayed greater cytotoxic ability than pNK (figure 5B). Importantly, unlike pNK cells, sNK cells did not show a significant decrease in cytotoxicity with IL-2 and anti-CD16 mAbs treatment (figure 5C). Next, we tested the IFN- γ secretion, one of the hallmarks of NK cells in modulating the TME, and found significant levels of IFN- γ was released in the supernatant of IL-2 treated sNK cells compared with IL-2 and anti-CD16 mAbs treated pNK cells (figure 5D), as well as the IFN- γ secretion in a single-cell manner using EliSpot (figure 5E), from sNK than those of pNK cells. Together, these data support that sNK cells mediate greater cytotoxicity and IFN- γ secretion levels than pNK cells. More

importantly, their functional proficiency is not hampered by split anergy induction.

sNK cells are polyfunctional

To explore the polyfunctionality of sNK cells, we employed the Isoplexis platform. Our results revealed that within the same treatment, individual sNK cells generated diverse soluble factors and were more polyfunctional than pNK cells (figure 6A). Additionally, a higher percentage of the sNK cell population exhibited polyfunctionality (ability to secretion more than one cytokine/chemokine per cell) compared with pNK cells when treated with IL-2 and anti-CD16 mAbs, or with sAJ2 bacterial preparation (figure 6B). When the polyfunctionality strength index (PSI) was calculated, sNK cells demonstrated higher PSI than pNK cells, particularly when treated with IL-2 and anti-CD16 mAbs (figure 6C). These findings collectively suggest that sNK cells possess a more comprehensive capacity in secreting effector cytokines and chemokines,

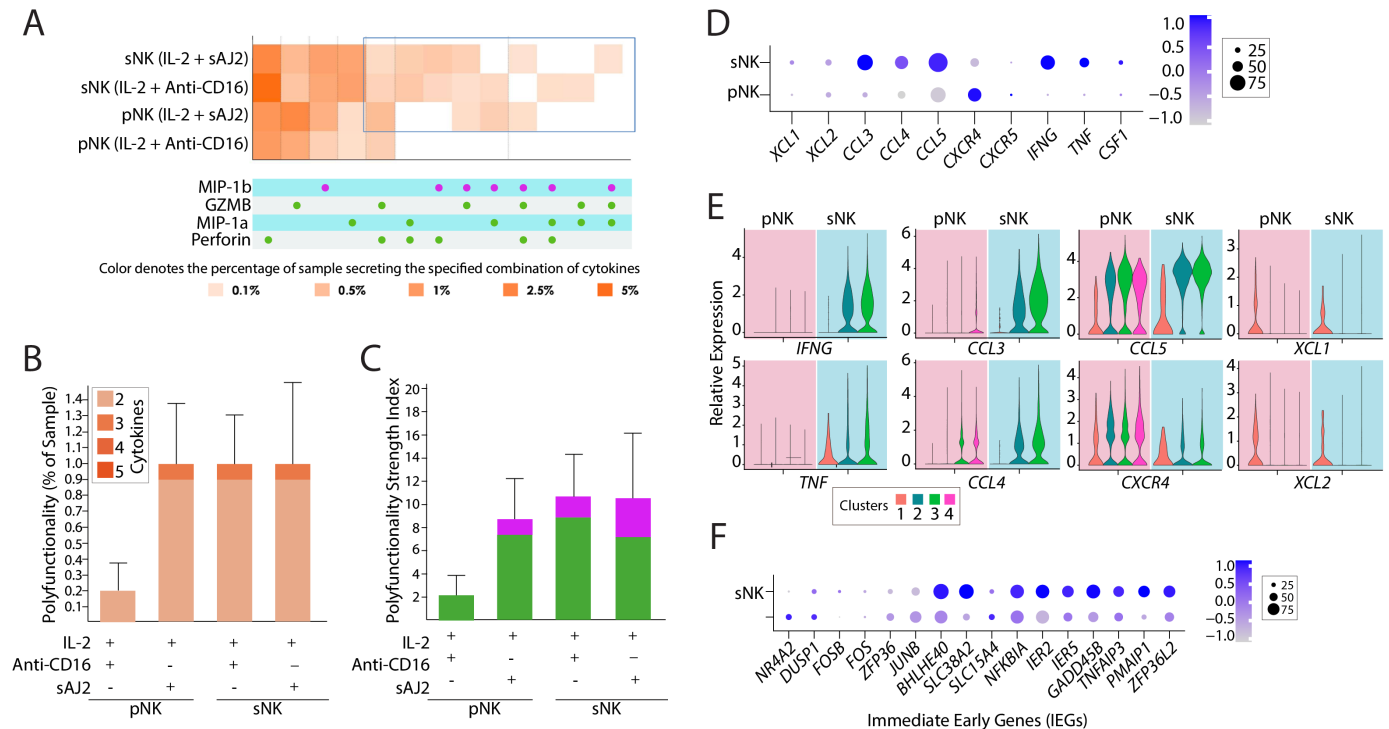


Figure 6 Supercharged natural killer (sNK) cells are more polyfunctional than primary NK cells. Both primary and sNK were treated with IL-2 and anti-CD16 mAb or sAJ2 and premarked approved (PMA) before using the PMA before using the commercial IsoCode Chip to measure the cytokine and chemokine secretion profile on per-cell basis. The polyfunctionality of NK cells is defined as two or more cytokines or chemokines secreted per cell. The overall profile of % NK cytokine secreting profile is shown as (A) a heatmap and (B) a bar graph. (C) Polyfunctional strength index is calculated as % polyfunctional cells multiplied by the intensities of the secreted cytokines/chemokine. (D) Relative transcript levels of chemokines and cytokines produced from pNK and sNK cells from single-cell RNA (scRNA-seq). (E) Violin plots indicate the relative expression of transcripts encoding cytokines and chemokines from pNK and sNK cells from scRNA-seq. (F) Relative transcript levels of immediate early genes in pNK and sNK cells from scRNA-seq. The size of the circle represents the percentage of transcript-positive cells, and the intensity of the colour indicates the transcript abundance.

exhibiting a greater polyfunctionality in secretion than pNK cells.

The transcriptional analysis further corroborates the augmented cytokine and chemokine secretion profile observed in sNK cells. Notably, at the gene expression level, a higher percentage of cells from sNK cells exhibit heightened expression of transcripts, including *CCL3*, *CCL4*, *CCL5*, *IFNG*, *TNF* and *CSF1*, in comparison to IL-2 treated pNK cells (figure 6D). These findings are consistent with the protein secretion data, further validating the enhanced functional capacity of sNK cells. Interestingly, the magnitude of upregulation of effector molecule gene expression varies across the different cell clusters within the sNK cell population, suggestive of different stages of developmental maturity (figure 6E). Additionally, immediate early gene expression, which has been linked to the early stages of cell activation and differentiation, was found to be upregulated in sNK cells, suggesting a potential mechanism underlying the increased effector cytokine and chemokine expression in this population (figure 6F). Collectively, the transcriptional analysis provides complementary evidence to the protein secretion data, underscoring the robust functional potential of sNK cells at both the transcriptome and protein levels.

sNK but not pNK cells were less inactivated after coculturing with tumour tissue

NK cells become CD16⁺CD56^{bright} phenotype after encountering an antigen, target cells or in tissue residence, similar to split anergy states.²³ Since sNK cells are not induced into split anergy with IL-2 and anti-CD16 antibody treatment, we sought to investigate if the same is true when they encounter tumour cells or tumour tissues. We cocultured the pNK or sNK cells with oral tumours derived from humanised BLT mice (figure 7A) and collected these NK cells for subsequent functional assays. Percent killing at various effector-target ratios (E:T ratio) and lytic unit 30/10⁶ cells (LU30/10⁶ cells) were quantified. Overall, sNK cells exhibited higher cytotoxicity than untreated or IL-2-treated pNK cells (figure 7B and online supplemental figure S5A–C). Untreated or IL-2-treated pNK cells demonstrated decreased cytotoxicity on coculture with tumour tissue (figure 7B and online supplemental figure S5A,B). A decrease in % cytotoxicity was observed in all three groups of NK cells after coculture with tumour tissue, with untreated pNK cells showing the highest decrease, followed by IL-2-treated pNK cells and sNK cells (figure 7E and online supplemental figure S5A–C). In summary, sNK cells demonstrated the highest

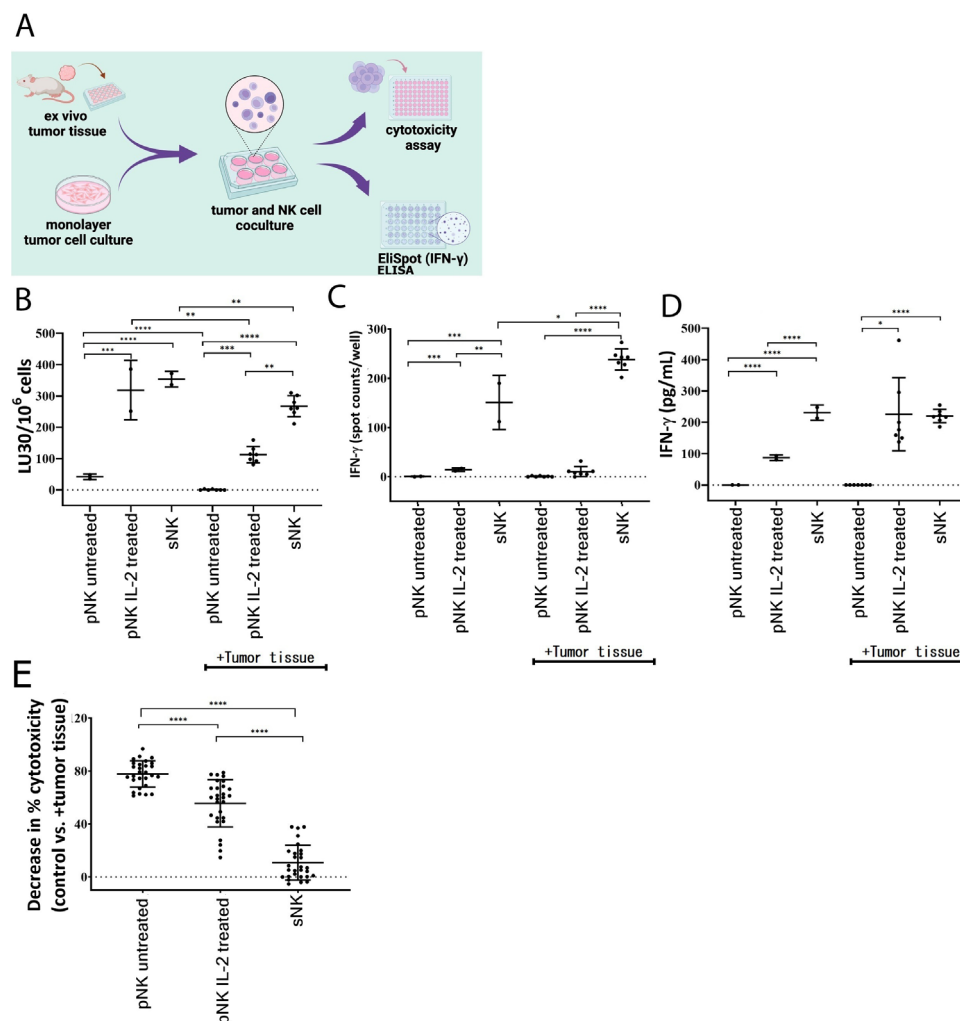


Figure 7 Primary natural killer (pNK) but not supercharged NK (sNK) cells were inactivated after coculturing with tumour tissue. (A) Schema for assessing the inactivation of pNK and sNK induced by tumour coculture. (B) Cytotoxicity of untreated pNK, IL-2-activated pNK and IL-2-activated sNK in the absence (control) and presence of (tumour tissues) cocultures were determined after the separation of NK cells from tumour tissues before using ⁵¹Cr release assay against OSCSCs, and the lytic unit 30/10⁶ cells (LU30/10⁶ cells) was calculated which denotes the number of NK cells required to lyse 30% of OSCSCs X100. (C) Untreated pNK, IL-2-activated pNK and IL-2-activated sNK in the absence (control) and presence of (tumour tissues) cocultures were performed and the NK cells were separated from tumour tissues to assess the number of IFN-γ spots in an Elispot assay. (D) Untreated pNK, IL-2-activated pNK and IL-2-activated sNK in the absence (control) and presence of (tumour tissues) cocultures were incubated overnight and the supernatants were recovered and subjected to ELISA for IFN-γ secretion. (E) Untreated pNK, IL-2-activated pNK and IL-2-activated sNK in the absence (control) and presence of (tumour tissue) cocultures were used to assess the decrease in cytotoxicity of NK cells after coculture with the tumour tissues as compared with their specific control NK cells. * (p-value < 0.01-0.05), ** (p-value < 0.01-0.001), *** (p-value < 0.001-0.0001), **** (p-value < 0.00001)

cytotoxicity among the three groups of NK cells, and their cytotoxic capacity was less compromised on encountering tumour tissue or single cell culture compared with pNK cells.

Besides the cytotoxicity, the NK cells harvested from the coculture were subsequently subjected to measuring their IFN-γ secretion ability (figure 7A). There was minimal secretion from the untreated pNK cells, as expected. IL-2-activated pNK and sNK cells demonstrated higher IFN-γ secretion when cocultured with tumour tissue (figure 7C,D and online supplemental figure S5D). We did not observe a significant difference in the IFN-γ secretion of sNK cells versus sNK+tumour tissue as seen

in figure 7D, possibly due to the plateau effect, sNK cells were already secreting significantly higher levels of IFN-γ so further increase was not detected by ELISA. Coupled with the reduced cytotoxicity, it is suggested that NK cells were induced into split anergy stage and switched into a cytokine-secreting mode when cultured with tumour tissue. However, sNK cells could maintain both their cytotoxic and IFN-γ secretion abilities, while cytotoxic function was inhibited in pNK cells with tumour tissue culture. These data support that, unlike pNK cells, sNK cells have superior functions against tumour cells and are not inactivated extensively after encountering tumours.

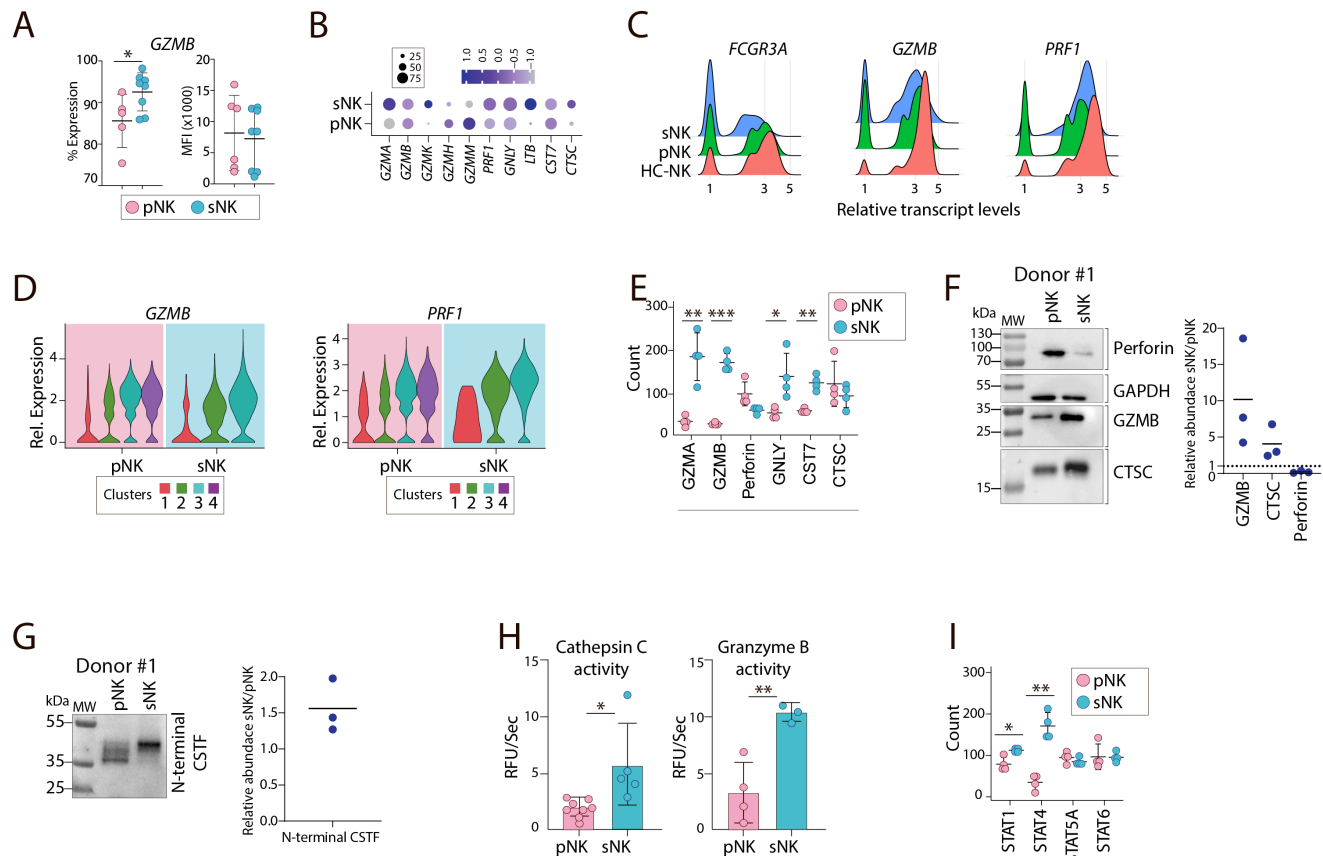


Figure 8 Post-translational regulation of GZMB activation by Cathepsin C results in superior cytotoxic potential of sNK cells. (A) Intracellular staining of GZMB. The per cent positive cells (left) and the mean fluorescence intensity (MFI). (B) Transcript levels of molecules involved in cytotoxicity from single-cell RNA (scRNA-seq) are presented as dot plots. The size of the circle represents the percentage of transcript-positive cells, and the intensity of the colour indicates the transcript abundance. (C) Transcript levels of *GZMB* and *PRF1* in sNK cells compared with pNK (IL-2-activated pNK) cells. (D) Violin plots representing the expression levels of *GZMB* and *PRF1* in individual NK clusters. (E) Protein levels of GZMs, *PRF1*, *GNLY*, *CST7* and *CTSC* from mass spectrometry analyses. (F) Proteomics data were validated using western blot and enzyme kinetics. Protein abundance of Perforin-1, Granzyme B and mature Cathepsin C in pNK and sNK cells derived from the same donors was analysed using western blot. (G) sNK cells appear to have more inactive CSTF (N-terminal CSTF). There is a considerable difference in the mobility of CSTF in sNK cells compared with pNK (IL-2-activated pNK) cells. Loading controls are shown in online supplemental figure S5. (H) Cathepsin C (left) and Granzyme B (right) are more active in sNK cells than pNK (IL-2-activated pNK) cells. (I) Protein quantities of *STAT1*, *STAT4*, *STAT5A* and *STAT6* from mass spectrometry analyses. *(p-value < 0.01-0.05), ***(p-value < 0.001-0.0001), ****(p-value < 0.0001).

Post-translational regulation of Granzyme B activation by Cathepsin C results in superior cytotoxic potential of sNK cells

To further understand the underlying mechanism of sNK cells not being split anergised by the IL-2 and anti-CD16 mAbs treatment and their profound cytotoxic ability, we first performed intracellular staining and found that Granzyme B expression is significantly increased in sNK cells, underlining a potential role in boosted tumour cell killing (figure 8A). To identify whether this increase is regulated at a transcriptional level, we analysed the transcript levels of cytotoxic molecules. We found *GZMA*, *GZMK*, *PRF1*, *GNLY* and *LTB* were relatively increased in sNK cells (figure 8B). However, the transcript levels of *GZMB* and *PRF1* remained largely comparable between HC-NK (untreated NK) and sNK cells (figure 8C). One possibility is that a unique subset among the total sNK cells could have upregulated *GZMB* and *PRF1*. To test this

possibility, we analysed their expression in individual clusters. We found the transcript levels of *GZMB* and *PRF1* were largely comparable between sNK and pNK (IL-2 treated pNK) cells in all the clusters (figure 8D).

Given there were no differences in the transcript levels, we next explored the protein expression levels of key molecules involved in the cytotoxicity using proteomic analysis. We found that Granzyme B protein expression was significantly increased in sNK cells, with Granzyme A and granzysin showing similar trends (figure 8E). Notably, Cathepsin C, a critical enzyme in the activation of Granzyme B, was present at similar levels in both sNK and pNK (IL-2 treated pNK) cells (figure 8E). However, Cystatin F (*CST7*), a Cathepsin C-targeting protease inhibitor, was significantly increased in sNK cells (figure 8E). Since proteomics data do not provide information on the functional status and posttranslational modifications,

we validated the data using western blots. The results confirmed increased Granzyme B protein expression and decreased active perforin-1 in sNK cells compared with pNK (IL-2 treated pNK) cells (figure 8F). Interestingly, mature Cathepsin C was found to be more abundant in sNK cells than pNK (IL-2 treated pNK) cells, in contrast to the proteomics data (figure 8F). Moreover, western blot analysis showed that expression of inactive dimeric Cystatin F, with intact N-terminal part, was increased in sNK cells (figure 8G and online supplemental figure S6A). The considerable differences in Cystatin F mobility between primary and sNK cells suggest differences in glycosylation (figure 8G and online supplemental figure S6B). Enzyme kinetics assay showed that Cathepsin C and Granzyme B activity were higher in sNK cells than in pNK (IL-2 treated pNK) cells (figure 8H). These findings suggest that while the proteomics data indicate that Cathepsin C and Cystatin F may suppress the cytotoxicity of sNK cells, they are post-translationally modified in a way that favours NK cell cytotoxicity.

Furthermore, we analysed important signal transducers and activators of transcription (STATs) in sNK cells. As a result, we found an elevated expression of STAT1 and STAT4, crucial regulators of IFN- γ production and NK cell-mediated cytotoxicity (figure 8I), supporting the augmented proliferation, cytokine production, and cytotoxicity capacity of sNK cells. In sum, these results suggest that the potent cytotoxic ability of sNK cells is due to their increased expression of Granzyme B and the posttranslational modification of Cystatin F and other cytotoxicity modulators, which leads to their resistance to the split anergy induction treatment and the inhibitory effect from cancer cells.

DISCUSSION

NK cells, with their immunosurveillance functions, have great potential to be clinically used. However, the major limitations include a lack of approaches to augment their antitumour effector functions and sustain their longevity in vivo. Previously, we established a method to significantly increase the antitumour functions of human NK cells, which we named sNK cells. The current study uses proteomic, transcriptomic and functional analyses to define the molecular mechanisms by which sNK cells function. We found that the sNK cells have upregulated the protein levels of activating/costimulatory receptors, decreased the expression of integrins required for tissue localisation, upregulated genes necessary for active proliferation, upregulated their capabilities to be polyfunctional and were not subjected to split anergy or exhaustion. We identify AP1 regulons-based transcriptional networks from single-cell transcriptomes responsible for the enhanced effector functions in sNK cells. We also define a post-translational mechanism that increases the activity of Granzyme B by interactions between Cathepsin C and Cystatin F.

Evidence supports that sNK cells are more active than primary NK cells. First, NK cell functions are governed by the interplay between activating and inhibitory receptors.³⁹ Both inhibitory and activating receptors are found elevated in sNK cells, including NKG2D, KIR2, NKp44, NKp46 and CD54 (ICAM-1), along with the decrease of CD62L, which is commonly observed in activated immune cells.^{40 41} CD16 and CD56 are two surface receptors to distinguish subsets of human NK cells: CD16⁺CD56^{dim} as cytotoxic NK cells and CD16⁺CD56^{Bright} as regulatory NK cells.^{42 43} It is worth noting that sNK cells exhibited higher CD56 and lower CD16 when compared with pNK cells, which is similar to the tissue-associated NK cell profile or split anergy induced with the combination of IL-2 and anti-CD16 mAbs in vitro, which have higher cytokine secretion ability and less cytotoxic function.^{1 42} We found a significant upregulation of SLAM family members CD2 and CD48. CD2 is the prototypical receptor for CD48, and their upregulation in sNK cells strongly suggests a *cis* or a *trans* interaction among sNK cells. Moreover, the pilus protein FimH from gram-positive *Escherichia coli* binds to CD48 expressed on macrophages and activates them,⁴⁴ indicating the potential possibility of a direct bacterial protein-mediated activation of sNK cells. Tetraspanin CD53 was upregulated in sNK cells as well. Homotypic interaction of CD53 between NK cells can augment their proliferation significantly,²⁹ providing a potential link between the upregulated costimulatory receptors and augmented cellular proliferation. Similarly, an increase in CD44, which binds to soluble or matrix-bound ligands, may also promote cell proliferation of sNK. CD59, a GPI-anchored glycoprotein also increased in sNK cells, is a co-receptor for NKP46 (NCR1) and NKP30 (NCR3) that augments NK cell-mediated cytotoxicity.³⁰

Moreover, a decrease in the protein levels of several integrins and their downstream signalling molecules indicated that the sNK cells are less motile with minimal actin cytoskeletal reorganisations. The variation of these proteins in sNK cells from pNK cells could be expected to alter cell morphology and behaviour, which coincide with the elongation and irregular shape of sNK cells and aggregation growth pattern observed in the culture. Aside from morphology and growth patterns, the modulation of cytoskeleton proteins also contributes to cell deformability, an essential process for cell proliferation. Along with the increase of proteins associated with deformability contributed by the downmodulation of the cytoskeleton, there are other standard markers for cell proliferation, which were also elevated, such as proliferating cell nuclear antigen, MKI67 and MCM. Our observations that MCM family members and other cell cycle-related proteins were increased in both proteomic and transcriptomic data strongly suggest and validate the increased proliferation of sNK cells. Of which the increase of MKI67 was confirmed with flow cytometric analysis. These observations tally with the fast proliferation rate of sNK cells reported previously,⁷ and the capability of rapid

expansion bestows large-scale production of sNK cells for cancer immunotherapy.

NK cells shape the tumour microenvironment through cytokine and chemokine secretion to potentiate tumour cells by mediating differentiation of CSCs, especially through secreted and membrane-bound IFN- γ and TNF- α , respectively.^{1 23 38 45} Most importantly, as previously established, differentiation of cancer cells enhances the sensitivity of these cells to chemotherapy, radiotherapy and immunotherapy.^{8 46} In bulk and single-cell analysis, sNK cells exhibited greater IFN- γ secretion than pNK cells. Moreover, multiplex analysis discovered that sNK cells possess a more diverse secretion profile, and single-cell profiling demonstrated that sNK cells are more polyfunctional than pNK cells. Positively, in the functional assays, with the same number of NK cells as tumour cells, supernatants from sNK cells were able to induce higher levels of differentiation to both pancreatic and oral stem-like cancer cells, which indicates that the application of sNK cells in cancer immunotherapy is essential to lay the foundation for the success of chemotherapy, radiotherapy and immunotherapy.

Furthermore, supernatants from sNK cells induced higher levels of cell death in both pancreatic and oral tumour cells, which might result from the high levels of IFN- γ and TNF- α , which are known as mechanisms that NK cells mediate cell lysis.^{47 48} We found AP1 regulons (ATF4, ATF3, JUN, MAFG) are exclusively present among the sNK cells compared with pNK cells, providing a molecular explanation for our findings. Importantly, the STAT1 regulon was also uniquely present in the sNK cells, which might be essential in regulating the effector functions. In addition, the protein levels of STAT4, which is known to increase chromatin accessibility to genes encoding both proinflammatory cytokines and factors involved in cytotoxicity, were also higher in the sNK cells. STAT4 is also known to function through the binding to the perforin gene promoter and cytokine secretion ability in response to IL-12 activation.^{49–51}

Even though sNK cells showed a CD56^{bright}CD16^{dim} profile, both flow cytometry and proteomic analysis revealed that sNK cells contained higher levels of Granzyme B. Indeed, in the 51-chromium release assay, when activated with IL-2, sNK cells exhibited much more profound cytotoxicity against stem-like oral tumour cells (OSCSCs) when compared with pNK cells. Interestingly, when attempting to induce split anergy in both primary and sNK cells with the combination of IL-2 and anti-CD16 mAb, only pNK cells showed a decrease in cytotoxicity. sNK cells, on the other hand, still retain significant cytotoxic functions against OSCSCs.

However, proteomic analysis revealed that in addition to Granzyme B, Cystatin F is also elevated in sNK cells, which has been reported to downregulate NK cell-mediated direct killing via the Perforin/Granzyme B pathway.⁵² Cystatin F inhibits the activity of Cathepsin C, which regulates the activation of Granzyme B by cleaving its pro-form.⁵² It has been reported that the expression

of both inactive dimeric and active monomeric forms of Cystatin F is increased in the split anergised NK cells, leading to a decrease in cytotoxicity against CSCs.²⁷ The Cystatin F protein level increase in sNK cells is rather unexpected. Both Cystatin F and Cathepsin C undergo various post-translational modifications that affect the function of these proteins. Cathepsin C is synthesised as a 60 kDa zymogen that undergoes proteolysis at multiple sites to release an internal propeptide. The resulting mature Cathepsin C monomer consists of three tightly linked subunits, a 16 kDa N-terminal exclusion domain, a 23 kDa catalytic heavy chain, and a 7.5 kDa light chain, held together by non-covalent interactions. Cystatin F must enter the lysosomes/cytotoxic granules to be activated to the monomeric form, which is able to inhibit Cathepsin C activity. The sorting of Cystatin F into the intracellular or extracellular compartments depends on the glycosylation status.^{27 53} However, due to sample preparation, using proteomics analysis, it is not possible to distinguish whether Cystatin F seen in sNK cells is activated to the monomeric form.

Western blot analysis showed that sNK cells express more of the inactive unprocessed form of Cystatin F. Moreover, the mobility of Cystatin F considerably differs in sNK cells compared with pNK cells, which is likely caused by the differences in glycosylation of Cystatin F in both cell types. Altered glycosylation greatly impacts the localisation of Cystatin F. It may prevent its trafficking to lysosomes/cytotoxic granules and, therefore, its ability to inhibit cathepsins.²⁷ This hypothesis aligns with the protein abundance we saw in primary and sNK cells derived from the same donors, revealing increased expression of the active forms of Granzyme B and Cathepsin C in sNK cells. Therefore, altered glycosylation of Cystatin F rather than its increased expression determines its impact on the cytotoxicity of sNK cells. The functional status of Cathepsin C and Granzyme B was analysed by enzyme kinetics, showing that both Cathepsin C and Granzyme B were more active in sNK cells than in pNK cells.

Regarding the augmented functions of sNK cells, they were used as immunotherapy in tumour-bearing humanised-BLT mice. In oral and pancreatic tumour models, tumour-derived from mice receiving sNK cells showed limited growth *ex vivo*. Additionally, the treatment with sNK cells enhances the frequency and the functions of CD8⁺ T cells and the host immunity in general, emphasising the promising potential of sNK cells in cancer immunotherapy.^{21 28} However, it has been suggested that the functions of NK cells are inactivated after encountering tumour cells.^{54 55} Therefore, the functionality of sNK cells was evaluated after they came across target cells.

Interestingly, the cytotoxic function of sNK cells remained the same despite coculture with tumour tissue or tumour cell culture. In contrast, pNK cells exhibited a major decrease in both scenarios. As mentioned earlier, the reduction in cytotoxicity might result from split anergy induction, where NK cells lose their cytotoxic function but gain great secretion ability.²³ As split anergy

of NK cells can be induced by blocking CD16 mAb, sNK cells may be unable to become split anergised as their CD16 was decreased on the cell surfaces. Consequently, the cytotoxicity is not decreased after meeting the target cells.

The reduced number and function of NK cells in cancer patients could lead to a lower success rate in developing adoptive treatment using autologous NK cells. To overcome this problem, we use allogeneic healthy donor-derived sNK cells (NK101). We have previously demonstrated the preclinical efficacy and safety of NK101 in tumour-bearing humanised-BLT mice. In a recently submitted paper, we presented the results of the first two cancer patients infused with NK101. The therapy demonstrated an excellent safety profile, with no adverse side effects or any discomfort to either patient postinfusion. Patients were monitored for 180 days post-therapy, and postinfusion blood analysis of patients revealed a positive early immune response in the absence of any kind of adverse safety events. Postinfusion clinical presentation revealed early signs of clinical efficacy, with several validated data points confirming NK101's ability to target and significantly decrease the tumour load in patients with cancer. The early clinical findings are consistent with preclinical results obtained using NK101 cells that demonstrated the ability to arrest tumour progression and restore immune function. In addition, we have submitted a pre-IND application and received a favourable response from the FDA, which we are in the process of submitting responses to the questions posed by the FDA. In addition, we have consistent expansion of greater than a billion sNK cells from primary NK cells, and therefore, it is quite easy to scale these cells up for clinical use.

In conclusion, the abilities of sNK cells, such as augmented proliferation, superior cytotoxic function, and proinflammatory cytokine production, and not being inactivated by tumour cells, confer significant potential in cancer immunotherapy.

MATERIALS AND METHODS

Cell lines, reagents and antibodies

RPMI 1650 (Gibco, Thermo Fisher Scientific, USA) complete medium with 10% fetal bovine serum (FBS) (Gemini Bio-Products, San Diego, USA) was used for immune cells and OSCCs and OSCSCs isolated from cancer patients with tongue tumour at UCLA.^{23 56} Alpha-MEM (Gibco, Thermo Fisher Scientific, USA) with 10% FBS was used for OCs cultures. RPMI 1650 complete medium with 10% human AB serum off the clot (Gemini Bio-Product, San Diego, USA) was used for sNK cell culture. RANKL and GM-CSF were purchased from PeproTech (New Jersey, USA), and recombinant human IL-2 was obtained from NIH-BRB. Anti-CD16 monoclonal antibodies were purchased from StemCell Technologies. Anti-human antibodies for CD45, CD3, CD16, CD56, CD14, NKG2D, KIR2, NKp44, NKp46, CD62L, Granzyme

B and Ki-67 to be used for flow cytometry were purchased from BioLegend (San Diego, USA).

Cell imaging

Images of NK cells were taken under $\times 400$ magnification using DMI6000 B inverted microscope and LAS X software (both Leica, Wetzlar, Germany).

Bacteria sonication

AJ2 is a combination of seven strains of Gram-positive probiotic bacteria (*Streptococcus thermophiles*, *Bifidobacterium longum*, *Bifidobacterium breve*, *Bifidobacterium infantis*, *Lactobacillus acidophilus*, *Lactobacillus plantarum* and *Lactobacillus paracasei*). AJ2 was resuspended in RPMI 1640 containing 10% FBS at 10 mg/mL. The bacterial suspension was then placed on ice, sonicated at 8 amplitude for 30 s, and rested for 15 s as a pulse. A sample of sonicated bacteria suspension would be taken and observed under the microscope. It was determined that the sonication was completed when greater than 80% of the cells had been lysed. The sonicated AJ2 (sAJ2) suspension was aliquoted and stored in a -80°C freezer for further use.

Purification of NK cells and monocytes from human PBMC

Peripheral blood was diluted with PBS. After Ficoll-Hypaque centrifugation, PBMC was harvested, washed and resuspended with RPMI for experiment or Robosep in desirable concentration for negative selection using EasySep human NK cell enrichment kit purchased from Stem Cell Technologies (Vancouver, BC, Canada). The purity of isolated NK cells was analysed by flow cytometric analysis. All cells were resuspended in RPMI 1640 complete medium.

Purification and generation of OCs from human PBMC

As described above, PBMCs were harvested from peripheral blood and were used for the negative selection of monocytes using the EasySep human monocyte enrichment kit purchased from Stem Cell Technologies (Vancouver, BC, Canada). Monocytes were resuspended into alpha-MEM with 1% autologous plasma. 50 million cells were plated per tissue culture dish with 151.9 cm^2 culture area and incubated at 37°C for 30 min. After incubation, floating cells were removed from the culture dish. Fresh alpha-MEM with 1% autologous plasma was replenished, and recombinant human macrophage colony-stimulating factor (25 ng/mL) (BioLegend, South Dakota, USA) was supplemented every 3 days, and RANKL (25 ng/mL) was supplemented every 3 days after day 6 for 21 days.

Generation of sNK cells

NK cells were purified from PBMC, as described above. Freshly isolated NK cells are treated with recombinant human IL-2 (rh-IL-2) (1000 U/mL) and anti-CD16 monoclonal antibody (3 $\mu\text{g/mL}$) (Biolegend) at 37°C for 16–18 hours. After the incubation time, NK cells are cocultured with OCs and sAJ2 (NK:OC:sAJ2 in 2:1:4 ratio)

(preparation as described above) at 37°C. The culture media were replenished every 3 days with rh-IL-2.⁷

Surface and intracellular staining, and flow cytometry analysis

1×10⁵ cells were used for each sample. All samples were stained with 100 µL of 1% BSA-PBS (Gemini Bio-Products, CA) and predetermined optimal concentration of desired fluorochrome (PE, FITC or PEcy5) conjugated antibodies and incubated at 4°C for 30 min. The sample was then washed and resuspended with 1% BSA-PBS. Intracellular staining was performed as described in the manufacturer's protocol. The sample was fixed with a fixation buffer for an hour in the dark at room temperature. A 2 mL of perm buffer was added to wash the sample, and the sample was centrifuged at 1400 rpm for 5 min. The washing step was repeated once, and the supernatants were discarded. Resuspended the sample in Perm buffer, added fluorochrome-conjugated antibody and incubated in the dark at room temperature for 30 min. Repeat the washing step with Perm buffer once and 1% BSA/PBS. Resuspend the sample with 1% BSA/PBS. The Epics C XL flow cytometer (Beckman Coulter, Pasadena, California, USA) and Attune NxT flow cytometer (Thermo Fisher Scientific, Waltham, Massachusetts, USA) were used. And FlowJo V.10.4 (BD, Oregon, USA) was used for analysis.

⁵¹Cr-release cytotoxicity assay

⁵¹Cr was purchased from Perkin Elmer (Santa Clara, California, USA). Standard 4-hour ⁵¹Cr release cytotoxicity assays were used to determine NK cytotoxic function in the experimental cultures and the sensitivities of target cells to NK-mediated cell lysis. Effector cells (1–2.5×10⁵ cells/well) were aliquoted into a 96-well round-bottom micro-well plate (Fisher Scientific, Pittsburgh, Pennsylvania, USA) and titrated at 4–6 serial dilutions with RPMI 1640. Target cells were labelled with 50 Ci ⁵¹Cr (Perkin Elmer, Santa Clara, California, USA) for an hour and excess ⁵¹Cr, then moved by washing with medium twice. ⁵¹Cr-labelled target cells (1×10⁴ per well) were aliquoted into a 96-well round-bottom micro-well plate containing effector cells at a top effector:target (E:T) ratio of 5:1. Plates were centrifuged and incubated for 4 hours. Following incubation, the supernatant was collected from each well into glass tubes and counted for released radioactivity using the gamma counter. Total release (⁵¹Cr-labelled target cells) and spontaneous release (supernatant harvested from wells containing only ⁵¹Cr-labelled target cells) values were measured to calculate the percentage specific cytotoxicity. The percentage-specific cytotoxicity was calculated by the following formula:

$$\% \text{ cytotoxicity} = \frac{\text{Experimental cpm} - \text{Spontaneous cpm}}{\text{Total cpm} - \text{Spontaneous cpm}} \times 100\%$$

Lytic unit 30 per million cells (LU30/10⁶ cells) was calculated using the inverse of the number of effector cells needed to lyse 30% of target cells×100.

ELISA

Human ELISA kits for IFN-γ (BioLegend, San Diego, USA) were used to detect the level of IFN-γ produced from cell cultures, respectively. The assay was conducted as described in the manufacturer's protocol. Briefly, 96-well EIA/RIA plates were coated with diluted capture antibody corresponding to target cytokine and incubated overnight at 4°C. After being washed four times with wash buffer (0.05% Tween20 in PBS), the coated plates were blocked with 1% BAS/PBS for an hour at room temperature on a shaker at 200 rpm. The plates were then washed again with wash buffer four times, and 100 µL of prepared standards or samples were added to the wells and incubated for 2 hours at room temperature on a plate shaker at 200 rpm. After incubation, the plates were washed four times with wash buffer, and 100 µL of detection antibody was added to each well, and the plates were incubated at room temperature for 1 hour on a shaker at 200 rpm. The plates were washed four times with wash buffer, loaded with Avidin-HRP solution, and incubated for 30 min at room temperature on the plate shaker at 200 rpm. After washing five times, 100 µL of TMB solution was added to each well, and the plates were incubated in the dark at room temperature until they developed a desired blue colour (or up to 15 min). Then, 100 µL of stop solution (2N H₂SO₄) was added to each well to stop the reaction. Finally, the plates were read at 450 nm to obtain absorbance values.

Enzyme-linked immunospot (ELISpot) assay

The ELISpot was conducted according to the manufacturer's instructions. Briefly, the plate was coated with primary antibody overnight at 4°C. After washing the plate with PBS twice, 50 000 cells/well were added into each well and incubated at 37°C for 16–18 hours. The plate was washed with PBS and wash buffer twice after the incubation period, and the detection antibody was added into each well and incubated at room temperature for 2 hours. After incubation, the plate was washed three times with wash buffer (0.05% Tween20/PBS). A tertiary solution was added to each well, and the plate was incubated at room temperature in the dark for 30 min. The plate was washed twice with wash buffer and twice with DI water before the blue development solution was added to each well and incubated for 15 min in the dark at room temperature. The reaction was stopped by gently rinsing the plate with water three times. And the plate was air-dried for 24 hours before being read. The number of IFN-γ secreting cells was analysed using Human IFN-γ Single-Color Enzymatic ELISPOT Assay, ImmunoSpot S6 UNIVERSAL analyser, and ImmunoSpot SOFTWARE (all CTL Europe, Bohn, Germany).

IsoPlexis single-cell secretome analysis

The polyfunctional secretome of primary and sNK cells was assessed using CodePlex single-cell cytokine profiling 32-plex (IsoPlexis, Branford, Connecticut, USA). NK cells were activated for 24 hours and added to a single-cell

barcoded chip with a 32-plex antibody array. After incubating for 16 hours, the signals for specific cytokines were measured and digitalised on a single-cell basis. Polyfunctionality of the cells is defined as more than one analyte tested found per cell. Polyfunctional strength index (PSI) is the percentage of polyfunctional cells in the total population multiplied by the mean fluorescence intensity of specific analytes tested.

Proteomic analysis

Cells were pelleted and reconstituted in buffer before being denatured by heat. Afterwards, samples were reduced, alkylated, trypsinised and incubated at 37°C overnight. Using Rappsilber's protocol,⁵⁷ samples were desalted, and a peptide bicinchoninic acid assay was performed. Samples were labelled using isobaric TMT tags and normalised to total protein before being pooled and desalted. Finally, the pooled sample was fractionated by high pH reverse phase and desalted before being injected into the Thermo Q Exactive Plus Orbitrap. Raw data were analysed via Proteome Discoverer 2.2. Protein–protein associations were identified using STRING analysis. Protein set enrichment analysis was performed with pathway databases from Gene Ontology, Reactome (clusterProfiler, V.4.2.2) and MSigDB (msigdb, V.7.5.1).⁵⁸ ggplot2 (V.3.3.6) was used to visualise log₂ fold changes in pathway enrichment between groups.

Oral tumour implantation in humanised BLT mice model

Combined immune-deficient NOD.CB17-Prkdcscid/J and NOD.Cg-Prkdcscid Il2rgtm1Wjl/SzJ (NSG mice lacking T, B and NK cells) were purchased from Jackson Laboratory and maintained in the animal facilities at UCLA in accordance with protocols approved by the UCLA animal research committee. Humanised-BLT (hu-BLT) mice were prepared on NSG background as previously described.⁵⁹ OSCSCs (0.5×10⁶ cells) were injected with 7 µL HC Matrigel (Corning, New York, USA) into the oral cavity (the floor of the mouth). Following the tumour implantation, the condition of the mice was monitored every day. Mice are euthanised when they start to show signs of morbidity, such as loss of weight, ruffled fur, hunched posture and immobility.^{21–28} The tumours were immediately cut into small chunks and frozen with 50% RPMI, 40% FBS and 10% DMSO for future use.

Cell culture of tissues from hu-BLT mice

Briefly, oral tumours were harvested from hu-BLT mice, cut into chunks and used for coculture experiments. Each tumour chunk was then cut into 1 mm³ pieces. The pieces were co-cultured with either untreated pNK or rh-IL-2 (1000 U/mL) treated pNK or sNK cells within RPMI 1640 medium supplemented with 10% FBS (Gemini BioProducts, CA), 1% antibiotics/antifungals, 1% sodium pyruvate and 1% non-essential amino acid MEM (Invitrogen, Life Technologies, California, USA) overnight. Then the supernatant was collected for ELISA, and the NK cells were used for Elispot, chromium release assay.

Statistical analysis

A paired or unpaired, two-tailed Student's t-test was performed for the statistical analysis using Prism-8 software (GraphPad Prism, California, USA). The following symbols represent the levels of statistical significance within each analysis: * (p<0.01–0.05), ** (p<0.01–0.001), *** (p<0.001). Graphical schema is generated with BioRender.com

Single-cell RNA library preparation and sequencing

Cells were loaded onto the 10X Chromium machine (10X Genomics) with a target capture of 8000 viable cells per sample. Library construction followed the manufacturer's protocols using the 10X Genomic Chromium Single Cell 3' Reagent Kit v3. Single-cell cDNA libraries were sequenced on an Illumina Novaseq 6000, with a depth of around 50 000 reads per cell to ensure robust data coverage.

Single-cell RNA data analysis

Following sequencing, raw data from each sample were demultiplexed. Subsequently, the reads were aligned to the 10X human reference genome, with 10X barcode and unique molecular identifier quantified using Cell Ranger (V.3.0.0, 10X Genomics) with default parameters. Aligned data were imported into R (V.4.1.1) using the Seurat package (V.4.3.0).⁶⁰ Cells comprising 250–6000 genes with 2%–15% mitochondrial components were selected for further analyses to ensure data quality. The SCTransformation method was employed for normalisation. Following normalisation, all datasets were integrated into a unified object based on the top 3000 gene features among datasets. A combination of principal components analysis and the Uniform Manifold Approximation and Projection dimensional reduction technique was applied to visualise the datasets in two dimensions. The top 30 principal components were selected to achieve unbiased clustering of single-cell datasets from all conditions. Dot plots and violin plots were generated using Seurat's in-built visualisation functions. Cell cycle heterogeneity was assessed by scoring cell cycle phases on each single cell. This scoring was based on 43 canonical S-phase markers and 54 canonical G2M-phase markers, with the remaining cells categorised as the G1 phase. A stacked bar plot was generated using ggplot2 (V.3.3.6) to visualise the distribution of cell cycle phases. GSEA was performed using ranked gene pathway databases from Gene ontology, Reactome (clusterProfiler, V.4.2.2) and MSigDB (msigdb, V.7.5.1).^{61–64} GSEA results were visualised using ggplot2 (V.3.3.6) to illustrate log₂ fold differences between conditions. Pseudotime trajectory analysis was conducted by using Monocle2 (V.2.22.0).⁶⁵ The pseudotime trajectory was constructed based on the top 25 genes in each cluster. All cells from the combined Seurat object were projected onto the trajectory with the DDRTree dimension reduction algorithm. The pseudotime heatmap,

showing dynamic changes in gene expression along the trajectory, was generated using the pheatmap package (V.1.0.12).

The SCENIC package (V.1.2.4) was employed for single-cell transcription factor inference, using the hg38 cisTarget databases from <https://resources.aertslab.org/cistarget/>.²³ Regulon activity results were further binarised, which is calculated with AUCell (V.1.16.0) for binarisation thresholds. The results were visualised using ComplexHeatmap (V.2.10.0) and ggplot2 (V.3.3.6).

Bulk RNA sequencing and data analysis

Primary and sNK cell samples were resuspended in TRIzol reagent (Invitrogen), and total RNA was extracted following the manufacturer's instruction. Library preparation and sequencing were performed at the MCW Genomic Sciences and Precision Medicine Centre. The cDNA library was prepared with NEBNext single cell/low input RNA library prep kit for Illumina (New England BioLabs). Libraries were sequenced via Novaseq 6000 (Illumina). Raw sequencing reads underwent processing using the nf-core/rnaseq pipeline (V.1.4.2) and were aligned to the GRCh38-3.0.0 reference genome.⁶⁶ The resulting gene expression matrix of the two samples was log2 transformed. The heatmap of selected transcripts was made with pheatmap (V.1.0.12).

Western blot analysis

Cells were washed twice with ice-cold PBS and lysed in NP-40 lysis buffer supplemented with a protease inhibitor cocktail (APEX-BIO). Lysates were centrifuged at 16 000 g at 4°C for 20 min to obtain post-nuclear cell fraction. Protein concentration was determined with a Pierce BCA protein assay kit (ThermoFisher Scientific). Non-reducing SDS-PAGE was performed, and separated proteins were transferred to the nitrocellulose membrane. Membranes were blocked for 1 hour in 5% non-fat dry milk in PBS. Membranes were incubated in primary antibodies overnight at 4°C and HRP-conjugated secondary antibodies for 1 hour at room temperature. Bands were visualised with Clarity Max Western ECL substrate (BioRad). Images were acquired with the ChemiDoc ML Imaging System (BioRad). Quantification analysis was done with Image Lab software. The following primary antibodies were used: mouse anti-Granzyme B (sc-8022, Santa Cruz Biotechnology), mouse anti-Cathepsin C (sc-74590, Santa Cruz Biotechnology), mouse anti-perforin-1 (sc-136994, Santa Cruz Biotechnology), rabbit anti-N-terminal part of Cystatin F (Amsbio) and rabbit anti-GAPDH for loading control (10494-I-AP, Proteintech). We used anti-rabbit HRP (111-035-045, Jackson ImmunoResearch) and anti-mouse HRP conjugated secondary antibodies (405 306 BioLegend). Some analyses were done using stain-free technology (BioRad).

Enzyme kinetics

Whole-cell lysates were prepared in citrate buffer (pH=6,2) with 1% Triton X-100 for Cathepsin C and 25 mM HEPES, pH 7.4 with 250 mM NaCl, 2.5 mM EDTA, 0.1% NP-40 for Granzyme B. Lysates were centrifuged at 16 000 g at 4°C for 20 min to obtain postnuclear cell fraction. Protein concentration was measured with the Pierce BCA protein assay. A 10 µg of proteins in whole cell lysates was activated in assay buffer 25 mM MES, 100 mM NaCl, pH=6, supplemented with 5 mM DTT for Cathepsin C or 50 mM Tris, 100 mM NaCl pH 7.4 for Granzyme B for 15 min. Substrate H- Gly-Phe-7-Amido-4-methylcoumarin (AMC) for Cathepsin C (70 µM, I-1220.0050, Bachem) or acetyl-Ile-Glu-Pro-Asp-AMC for Granzyme B (50 µM, I-1835.0005, Bachem) was added and formation of fluorescent degradation products was measured continuously at excitation of 470 nm and emission at 460 nm on microplate reader BioTek Synergy H1. Protease activities are expressed as the rate of AMC release over time.

Author affiliations

¹Division of Oral Biology and Medicine, The Jane and Jerry Weintraub Center for Reconstructive Biotechnology, University of California Los Angeles School of Dentistry, Los Angeles, California, USA

²Department of Microbiology and Immunology, Medical College of Wisconsin, Milwaukee, Wisconsin, USA

³Division of Hematology and Oncology, Department of Medicine, Medical College of Wisconsin, Milwaukee, Wisconsin, USA

⁴Department of Biotechnology, Jožef Stefan Institute, Ljubljana, Slovenia

⁵Faculty of Pharmacy, University of Ljubljana, Ljubljana, Slovenia

⁶Semel Institution, University of California Los Angeles, Los Angeles, California, USA

⁷The Jonsson Comprehensive Cancer Center, University of California Los Angeles School of Dentistry, Los Angeles, California, USA

Acknowledgements The work is based on the first author's thesis 'Ko, M. (2021). Osteoclast-induced supercharged NK cells preferentially select and expand CD8+ T cells, differences with primary NK cells and the fold of CD16 receptors on NK activation. UCLA. ProQuest ID: Ko_ucla_0031D_19492. Merritt ID: ark:/13030/m5k7088z. Retrieved from <https://escholarship.org/uc/item/86t5n8pn>'.

Contributors M-WK: designed and performed the experiments, data analysis, and wrote and edited the manuscript. AM performed the experiments and computational analysis. ES, MPN, LWG, PW, P-CP and WC performed the experiments and data analysis. JPW and JK reviewed the manuscript. KK performed data analysis and figure preparation of figure 7 and online supplemental figures and edited the manuscript. SM and AJ designed the experiments and reviewed and edited the manuscript. AJ is responsible for the overall content as guarantor.

Funding R01AI183571 (SM); Nicholas Family Foundation (SM); Gardetto Family's Everyday Good Foundation (SM) and Nan Gardetto Endowed Chair (SM) and AHW & Cancer Center of MCW (SM). Slovenian Research and Innovation Agency grants: P4-0127 (JK), Z3-50102 (ES), J3-60067 (MPN).

Competing interests None declared.

Patient and public involvement Patients and/or the public were not involved in the design, or conduct, or reporting, or dissemination plans of this research.

Patient consent for publication Not applicable.

Ethics approval The study and procedures were approved by the UCLA Institutional Review Board (IRB) (IRB#11-000781), and all participants signed written informed consent per the Declaration of Helsinki. Animal research was performed under the written approval of the UCLA Animal Research Committee (ARC) (protocol #2012-101-13) in accordance with all federal, state and local guidelines.

Provenance and peer review Not commissioned; externally peer reviewed.

Data availability statement No data are available.

Supplemental material This content has been supplied by the author(s). It has not been vetted by BMJ Publishing Group Limited (BMJ) and may not have been peer-reviewed. Any opinions or recommendations discussed are solely those of the author(s) and are not endorsed by BMJ. BMJ disclaims all liability and responsibility arising from any reliance placed on the content. Where the content includes any translated material, BMJ does not warrant the accuracy and reliability of the translations (including but not limited to local regulations, clinical guidelines, terminology, drug names and drug dosages), and is not responsible for any error and/or omissions arising from translation and adaptation or otherwise.

Open access This is an open access article distributed in accordance with the Creative Commons Attribution Non Commercial (CC BY-NC 4.0) license, which permits others to distribute, remix, adapt, build upon this work non-commercially, and license their derivative works on different terms, provided the original work is properly cited, appropriate credit is given, any changes made indicated, and the use is non-commercial. See: <http://creativecommons.org/licenses/by-nc/4.0/>.

ORCID iD

Kawaljit Kaur <http://orcid.org/0000-0003-1936-5985>

REFERENCES

- Jewett A, Man YG, Tseng HC. Dual functions of natural killer cells in selection and differentiation of stem cells; role in regulation of inflammation and regeneration of tissues. *J Cancer* 2013;4:12–24.
- Abel AM, Yang C, Thakar MS, et al. Natural Killer Cells: Development, Maturation, and Clinical Utilization. *Front Immunol* 2018;9:1869.
- Clement MV, Haddad P, Soulie A, et al. Involvement of granzyme B and perforin gene expression in the lytic potential of human natural killer cells. *Nouv Rev Fr Hematol* (1978) 1990;32:349–52.
- Jewett A, Kos J, Kaur K, et al. Natural Killer Cells: Diverse Functions in Tumor Immunity and Defects in Pre-neoplastic and Neoplastic Stages of Tumorigenesis. *Mol Ther Oncolytics* 2020;16:41–52.
- Kaur K, Nanut MP, Ko M-W, et al. Natural killer cells target and differentiate cancer stem-like cells/undifferentiated tumors: strategies to optimize their growth and expansion for effective cancer immunotherapy. *Curr Opin Immunol* 2018;51:170–80.
- Wang H, Zeng Y, Zhang M, et al. CD56^{bright}CD16⁺ natural killer cells are shifted toward an IFN- γ -promoting phenotype with reduced regulatory capacity in osteoarthritis. *Hum Immunol* 2019;80:871–7.
- Kaur K, Cook J, Park S-H, et al. Novel Strategy to Expand Super-Charged NK Cells with Significant Potential to Lyse and Differentiate Cancer Stem Cells: Differences in NK Expansion and Function between Healthy and Cancer Patients. *Front Immunol* 2017;8:297.
- Kozłowska AK, Topchyan P, Kaur K, et al. Differentiation by NK cells is a prerequisite for effective targeting of cancer stem cells/poorly differentiated tumors by chemopreventive and chemotherapeutic drugs. *J Cancer* 2017;8:537–54.
- Kaur K, Chang H-H, Cook J, et al. Suppression of Gingival NK Cells in Precancerous and Cancerous Stages of Pancreatic Cancer in KC and BLT-Humanized Mice. *Front Immunol* 2017;8:1606.
- Liu E, Marin D, Banerjee P, et al. Use of CAR-Transduced Natural Killer Cells in CD19-Positive Lymphoid Tumors. *N Engl J Med* 2020;382:545–53.
- Terranova-Barberio M, Pawłowska N, Dhawan M, et al. Exhausted T cell signature predicts immunotherapy response in ER-positive breast cancer. *Nat Commun* 2020;11:3584.
- Chen EX, Jonker DJ, Loree JM, et al. Effect of Combined Immune Checkpoint Inhibition vs Best Supportive Care Alone in Patients With Advanced Colorectal Cancer: The Canadian Cancer Trials Group CO.26 Study. *JAMA Oncol* 2020;6:831–8.
- Rosenberg SA, Restifo NP. Adoptive cell transfer as personalized immunotherapy for human cancer. *Science* 2015;348:62–8.
- Sharma P, Allison JP. The future of immune checkpoint therapy. *Science* 2015;348:56–61.
- Liem NT, Van Phong N, Kien NT, et al. Phase I Clinical Trial Using Autologous Ex Vivo Expanded NK Cells and Cytotoxic T Lymphocytes for Cancer Treatment in Vietnam. *Int J Mol Sci* 2019;20:3166.
- Leivas A, Perez-Martinez A, Blanchard MJ, et al. Novel treatment strategy with autologous activated and expanded natural killer cells plus anti-myeloma drugs for multiple myeloma. *Oncoimmunology* 2016;5:e1250051.
- Lee JH, Lee J-H, Lim Y-S, et al. Adjuvant immunotherapy with autologous cytokine-induced killer cells for hepatocellular carcinoma. *Gastroenterology* 2015;148:1383–91.
- Miller JS, Soignier Y, Panoskaltsis-Mortari A, et al. Successful adoptive transfer and in vivo expansion of human haploidentical NK cells in patients with cancer. *Blood* 2005;105:3051–7.
- Sakamoto N, Ishikawa T, Kokura S, et al. Phase I clinical trial of autologous NK cell therapy using novel expansion method in patients with advanced digestive cancer. *J Transl Med* 2015;13:277.
- Judge SJ, Yanagisawa M, Sturgill IR, et al. Blood and tissue biomarker analysis in dogs with osteosarcoma treated with palliative radiation and intra-tumoral autologous natural killer cell transfer. *PLoS One* 2020;15:e0224775.
- Kaur K, Topchyan P, Kozłowska AK, et al. Super-charged NK cells inhibit growth and progression of stem-like/poorly differentiated oral tumors *in vivo* in humanized BLT mice; effect on tumor differentiation and response to chemotherapeutic drugs. *Oncoimmunology* 2018;7:e1426518.
- Malarkannan S. Missing-self: revisited. *Semin Immunol* 2006;18:143–4.
- Tseng H-C, Bui V, Man Y-G, et al. Induction of Split Anergy Conditions Natural Killer Cells to Promote Differentiation of Stem Cells through Cell-Cell Contact and Secreted Factors. *Front Immunol* 2014;5:269.
- Perišić Nanut M, Sabotić J, Švajger U, et al. Cystatin F Affects Natural Killer Cell Cytotoxicity. *Front Immunol* 2017;8:1459.
- Prunk M, Nanut MP, Sabotić J, et al. Increased cystatin F levels correlate with decreased cytotoxicity of cytotoxic T cells. *Radiol Oncol* 2019;53:57–68.
- Prunk M, Perišić Nanut M, Jakoš T, et al. Extracellular Cystatin F Is Internalised by Cytotoxic T Lymphocytes and Decreases Their Cytotoxicity. *Cancers (Basel)* 2020;12:3660.
- Senjor E, Pirro M, Švajger U, et al. Different glycosylation profiles of cystatin F alter the cytotoxic potential of natural killer cells. *Cell Mol Life Sci* 2023;81:8.
- Kaur K, Kozłowska AK, Topchyan P, et al. Probiotic-Treated Super-Charged NK Cells Efficiently Clear Poorly Differentiated Pancreatic Tumors in Hu-BLT Mice. *Cancers (Basel)* 2019;12:63.
- Todros-Dawda I, Kveberg L, Vaage JT, et al. The tetraspanin CD53 modulates responses from activating NK cell receptors, promoting LFA-1 activation and dampening NK cell effector functions. *PLoS One* 2014;9:e97844.
- Marcenaro E, Augugliaro R, Falco M, et al. CD59 is physically and functionally associated with natural cytotoxicity receptors and activates human NK cell-mediated cytotoxicity. *Eur J Immunol* 2003;33:3367–76.
- Yang C, Siebert JR, Burns R, et al. Heterogeneity of human bone marrow and blood natural killer cells defined by single-cell transcriptome. *Nat Commun* 2019;10:3931.
- Crinier A, Milpied P, Escalière B, et al. High-Dimensional Single-Cell Analysis Identifies Organ-Specific Signatures and Conserved NK Cell Subsets in Humans and Mice. *Immunity* 2018;49:971–86.
- Friedman N, Ninio M, Pe'er I, et al. A structural EM algorithm for phylogenetic inference. *J Comput Biol* 2002;9:331–53.
- Aibar S, González-Blas CB, Moerman T, et al. SCENIC: single-cell regulatory network inference and clustering. *Nat Methods* 2017;14:1083–6.
- Wu Z, Nicoll M, Ingham RJ. AP-1 family transcription factors: a diverse family of proteins that regulate varied cellular activities in classical hodgkin lymphoma and ALK+ ALCL. *Exp Hematol Oncol* 2021;10:4.
- Gallardo E, de Andrés I, Illa I. Cathepsins are upregulated by IFN- γ /STAT1 in human muscle culture: a possible active factor in dermatomyositis. *J Neuropathol Exp Neurol* 2001;60:847–55.
- Raulet DH. Missing self recognition and self tolerance of natural killer (NK) cells. *Semin Immunol* 2006;18:145–50.
- Jewett A, Man Y, Cacalano N, et al. Natural killer cells as effectors of selection and differentiation of stem cells: role in resolution of inflammation. *J Immunotoxicol* 2014;11:297–307.
- Pegram HJ, Andrews DM, Smyth MJ, et al. Activating and inhibitory receptors of natural killer cells. *Immunol Cell Biol* 2011;89:216–24.
- Lin S-J, Chang L-Y, Yan D-C, et al. Decreased intercellular adhesion molecule-1 (CD54) and L-selectin (CD62L) expression on peripheral blood natural killer cells in asthmatic children with acute exacerbation. *Allergy* 2003;58:67–71.
- Yang S, Liu F, Wang QJ, et al. The shedding of CD62L (L-selectin) regulates the acquisition of lytic activity in human tumor reactive T lymphocytes. *PLoS One* 2011;6:e22560.
- Vitale M, Della Chiesa M, Carlomagno S, et al. The small subset of CD56^{bright}CD16⁺ natural killer cells is selectively responsible for both cell proliferation and interferon-gamma production upon interaction with dendritic cells. *Eur J Immunol* 2004;34:1715–22.
- Poli A, Michel T, Thérésine M, et al. CD56^{bright} natural killer (NK) cells: an important NK cell subset. *Immunology* 2009;126:458–65.
- McArdel SL, Terhorst C, Sharpe AH. Roles of CD48 in regulating immunity and tolerance. *Clin Immunol* 2016;164:10–20.

- 45 Tseng HC, Cacalano N, Jewett A. Split anergized Natural Killer cells halt inflammation by inducing stem cell differentiation, resistance to NK cell cytotoxicity and prevention of cytokine and chemokine secretion. *Oncotarget* 2015;6:8947–59.
- 46 Lanzon CJ. *Strategies to target pancreatic cancer stem cells using natural killer cells and chemotherapeutic drugs*. Vol 56. . Los Angeles: University of California, 2015:1.
- 47 Arase H, Arase N, Saito T. Fas-mediated cytotoxicity by freshly isolated natural killer cells. *J Exp Med* 1995;181:1235–8.
- 48 Wu AJ, Chen ZJ, Tsokos M, *et al*. Interferon-gamma induced cell death in a cultured human salivary gland cell line. *J Cell Physiol* 1996;167:297–304.
- 49 Gotthardt D, Sexl V. STATs in NK-Cells: The Good, the Bad, and the Ugly. *Front Immunol* 2016;7:694.
- 50 Thierfelder WE, van Deursen JM, Yamamoto K, *et al*. Requirement for Stat4 in interleukin-12-mediated responses of natural killer and T cells. *Nature New Biol* 1996;382:171–4.
- 51 Yamamoto K, Shibata F, Miyasaka N, *et al*. The human perforin gene is a direct target of STAT4 activated by IL-12 in NK cells. *Biochem Biophys Res Commun* 2002;297:1245–52.
- 52 Perišić Nanut M, Sabotić J, Jewett A, *et al*. Cysteine cathepsins as regulators of the cytotoxicity of NK and T cells. *Front Immunol* 2014;5:616.
- 53 Colbert JD, Plechanovová A, Watts C. Glycosylation directs targeting and activation of cystatin f from intracellular and extracellular sources. *Traffic* 2009;10:425–37.
- 54 Jewett A, Bonavida B. Target-induced inactivation and cell death by apoptosis in a subset of human NK cells. *J Immunol* 1996;156:907–15.
- 55 Jewett A, Tseng HC. Tumor induced inactivation of natural killer cell cytotoxic function; implication in growth, expansion and differentiation of cancer stem cells. *J Cancer* 2011;2:443–57.
- 56 Tseng H-C, Arasteh A, Paranjpe A, *et al*. Increased lysis of stem cells but not their differentiated cells by natural killer cells; de-differentiation or reprogramming activates NK cells. *PLoS One* 2010;5:e11590.
- 57 Rappsilber J, Mann M, Ishihama Y. Protocol for micro-purification, enrichment, pre-fractionation and storage of peptides for proteomics using StageTips. *Nat Protoc* 2007;2:1896–906.
- 58 Grigorieva J, Asmellash S, Net L, *et al*. Mass Spectrometry-Based Multivariate Proteomic Tests for Prediction of Outcomes on Immune Checkpoint Blockade Therapy: The Modern Analytical Approach. *Int J Mol Sci* 2020;21:838.
- 59 Wege AK, Melkus MW, Denton PW, *et al*. Functional and phenotypic characterization of the humanized BLT mouse model. *Curr Top Microbiol Immunol* 2008;324:149–65.
- 60 Butler A, Hoffman P, Smibert P, *et al*. Integrating single-cell transcriptomic data across different conditions, technologies, and species. *Nat Biotechnol* 2018;36:411–20.
- 61 Fabregat A, Jupe S, Matthews L, *et al*. The Reactome Pathway Knowledgebase. *Nucleic Acids Res* 2018;46:D649–55.
- 62 Subramanian A, Tamayo P, Mootha VK, *et al*. Gene set enrichment analysis: a knowledge-based approach for interpreting genome-wide expression profiles. *Proc Natl Acad Sci U S A* 2005;102:15545–50.
- 63 Ashburner M, Ball CA, Blake JA, *et al*. Gene ontology: tool for the unification of biology. The Gene Ontology Consortium. *Nat Genet* 2000;25:25–9.
- 64 Liberzon A, Birger C, Thorvaldsdóttir H, *et al*. The Molecular Signatures Database (MSigDB) hallmark gene set collection. *Cell Syst* 2015;1:417–25.
- 65 Qiu X, Hill A, Packer J, *et al*. Single-cell mRNA quantification and differential analysis with Censur. *Nat Methods* 2017;14:309–15.
- 66 Ewels PA, Peltzer A, Fillinger S, *et al*. The nf-core framework for community-curated bioinformatics pipelines. *Nat Biotechnol* 2020;38:276–8.